Zeitschrift: Eclogae Geologicae Helvetiae
Herausgeber: Schweizerische Geologische Gesellschaft
Band: 91 (1998)
Heft: 1

Artikel: Biostratigraphy, mineralogy and geochemistry of the Trabakua Pass and Ermua sections in Spain : Paleocene-Eocene transitions

Autor: Bolle, Marie-Pierre / Adatte, Thierry / Keller, Gerta

DOI: https://doi.org/10.5169/seals-168405

0012-9402/98/010001-25 $1.50 + 0.20/0
Birkhäuser Verlag, Basel, 1998

Eclogae geol. Helv. 91 (1998) 1–25

Biostratigraphy, mineralogy and geochemistry of the Trabakua Pass and Ermua sections in Spain: Paleocene-Eocene transition

MARIE-PIERRE BOLLE[1], THIERRY ADATTE[1], GERTA KELLER[2], KATHARINA VON SALIS[3] & JOHANNES HUNZIKER[4]

Key words: Paleocene-Eocene transition, Basque Basin, potential stratotype, planktic foraminifera, calcareous nannofossils, stable isotopes, clay-minerals, geochemistry

ABSTRACT

Isotopic, geochemical and bulk mineralogical analyses in the Trabakua and Ermua sections, Basque Basin, reveal major changes across the Paleocene-Eocene transition. Expanded sedimentary records exhibit a gradual decrease of 1.0 ‰ in $\delta^{13}C$ values in the lower part of Zone P5 followed by a more rapid 3 ‰ negative excursion. The 3 ‰ $\delta^{13}C$ excursion is associated with an abrupt decrease in carbonate sedimentation, increased detrital flux and decreased grain size which suggest changes in marine/atmospheric currents and/or size and structure of the ocean carbon reservoir. The clays recognized at Trabakua record a deep burial diagenesis as indicated by two generations of chlorite, the presence of mixed-layers chlorite-smectite and illite-smectite, the absence of smectite and the near absence of kaolinite. The very low $\delta^{18}O$ values (< -3.5‰) throughout the Trabakua and Ermua sections reflect diagenetic alteration rather than paleotemperatures. Because of deep burial diagenesis and very poorly preserved microfossils, the Trabakua Pass and Ermua sections are not optimal potential stratotypes for the Paleocene-Eocene boundary.

RESUME

Différentes analyses, faunistiques, minéralogiques, isotopiques et géochimiques, effectuées sur des sédiments provenant des profils de Trabakua et Ermua localisés dans le pays basque espagnol montrent des changements majeurs à la transition Paléocène-Eocène. Cette dernière est marquée lithologiquement par un intervalle argileux d'une épaisseur de 3 mètres. La transition Paléocène-Eocène est caractérisée par une diminution graduelle de 1‰ du $\delta^{13}C$ dans la partie inférieure de la Zone P5, suivie par une excursion négative abrupte de 3 ‰ du $\delta^{13}C$. Cette excursion négative est associée à une importante diminution de la sédimentation carbonatée, une augmentation des apports détritiques ainsi qu'à une réduction de la taille des particules. Ces changements suggèrent une diminution de la productivité biologique primaire ainsi que des variations dans la source des sédiments et/ou des courants océaniques/atmosphériques. Deux générations de chlorite, la présence d'interstratifiés illite-smectite et chlorite-smectite, ainsi que l'absence de smectite et kaolinite indiquent que les sédiments de Trabakua ont subi une diagenèse importante. En raison de la mauvaise préservation des microfossiles et de la diagenèse qui affecte les sédiments, le choix combiné des profils de Trabakua et Ermua comme stratotype de la limite Paléocène – Eocène ne serait pas optimal.

Introduction

The Paleocene-Eocene transition is characterized by a 6-8° warming in the deep ocean and high latitude surface ocean as indicated by foraminiferal $\delta^{18}O$ analyses and by a major change in the carbon budget as indicated by a negative excursion of 2.5–3‰ in carbonate $\delta^{13}C$ values (Kennett & Stott 1991; Koch et al. 1992; Pak & Miller 1992; Stott 1992; Lu & Keller 1993; Bralower et al. 1995; Canudo et al. 1995; Lu et al. 1996; Thomas & Shackleton 1996; Stott et al. in press). Clay mineral associations suggest a time of exceptionally high precipitation on Antarctica (Robert & Kennett 1994), but an arid climate in the Tethys region (Adatte et al. 1995). Coincident with the negative $\delta^{13}C$ excursion, carbonate sedimentation decreased drastically in all major basins as well as on continental margins (O 'Connell 1990; Canudo et al. 1995; Thomas & Shackleton 1996), indicating significant changes in ocean chemistry which might have affected atmospheric CO_2 concentrations. The reorganization of ecosystems associated with the P-E global change is marked by a mass extinction in benthic foraminifera known as the benthic extinction event (BEE) (Miller et al. 1987; Thomas 1990; Katz & Miller 1991; Pak & Miller 1992; Speijer 1994a, 1994b; Canudo et al. 1995; Thomas & Shackleton 1996), and the radiation and proliferation of

[1] Institut de Géologie, 11 Emile-Argand, Université de Neuchâtel, CH–2007 Neuchâtel. marie-pierre.bolle@geol.unine.ch
[2] Dpt of Geosciences, Princeton University, Princeton, USA–NJ 08544
[3] Geologisches Institut, ETH-Zentrum, CH–8092 Zürich
[4] Institut de Minéralogie et Pétrographie, BFSH2, Université de Lausanne, CH–1015 Lausanne

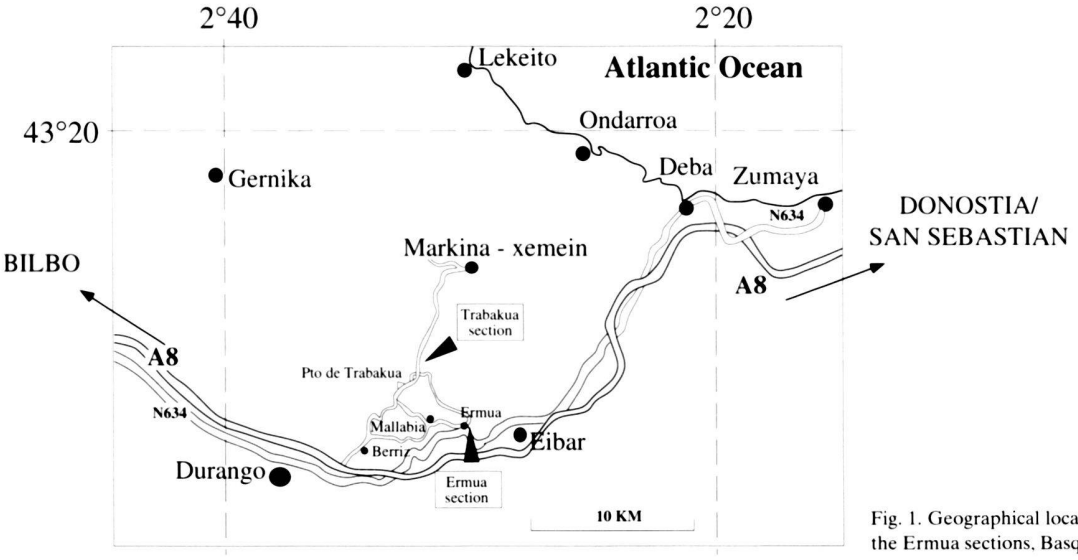

Fig. 1. Geographical location of the Trabakua Pass and the Ermua sections, Basque Basin, North of Spain.

thermophilic species in marine plankton and terrestrial vertebrates and plants (Gingerich 1980, 1986; Wing et al. 1991; Axelrod 1992; Wing & Greenwood 1993; Lu & Keller 1993, 1995a, 1995b).

The Tethys is generally considered as a crucial region for investigating the potential cause(s) and mechanism(s) of the global P-E change (Kennett & Stott 1990, 1991; Lu et al. 1996). During the P-E transition, the Tethys was a semi-restricted basin surrounded by vast shallow epicontinental seas and undergoing intense tectonic activity (Oberhänsli & Hsü 1986; Klootwijk et al. 1992; Oberhänsli 1992; Selverstone & Gutzler 1993). These unique geographic and tectonic features suggest that the Tethys region was most likely a major source and/or sink of organic carbon (Raymo & Ruddiman 1992; Selverstone & Gutzler 1993) and potentially a major source of warm saline deep water (Kennett & Stott 1990, 1991), two conditions that are probably the primary driving forces for the P-E global climatic and environmental changes (Lu et al. 1996).

The Trabakua Pass section has been proposed by Coccioni et al. (1994) and Orue-Etxebarria et al. (1996) as potential stratotype section for the Paleocene/Eocene boundary. According to these authors, this section fullfils most of the requirements for a stratotype section as suggested by the International Commission on Stratigraphy (Remane et al. 1997): a) easy access, b) hemipelagic sedimentation, c) continuous, if somewhat condensed, sedimentation across the boundary, d) absence of synsedimentary and tectonic disturbances, e) absence of diagenetic alteration or redeposition, f) abundance and diversity of well preserved fossils, and g) good magnetostratigraphic and isotopic records. Moreover, this section can be correlated with the Ermua section, located about 10 km to the south of the study area which shows resedimented deposits from a coeval carbonate platform. The proposed boundary section offers therefore the possibility to intercalibrate the biostratigraphic scales of the most important deep and shallow marine fossil groups across the Paleocene/Eocene boundary (Orue-Etxebarria et al. 1996).

To evaluate the Trabakua Pass section as potential P-E boundary stratotype, we conducted a detailed investigation of mineralogical, geochemical, isotopic and faunal changes across the P-E transition of the Trabakua Pass and Ermua sections. The main objectives of this study are: 1) to test the choice of the Trabakua Pass section as potential stratotype with the aid of mineralogical, chemical and isotopic data. 2) To confirm the correlation, based on biostratigraphic data between the two sections. And 3) to correlate this section with others located in the Tethyan realm (Alamedilla, Caravaca).

Location and paleogeographical setting

The Trabakua Pass and Ermua sections are located in the northwestern part of the Pyrenees (Basque Region) of northern Spain and can be reached by the road from Bilbo to Durango (Fig. 1). The Ermua section is located near the village of Ermua and the Trabakua Pass section is 1 km north of the Trabakua Pass.

During the late Cretaceous to early Eocene, the Basque Basin in which the Trabakua and Ermua sections are located, was an interplate trough of intermediate water depth (Plaziat 1981; Pujalte et al. 1992, 1993, 1994). This basin was elongated in a E-W direction, opening westward into the Bay of Biscay, and surrounded by shallow shelf areas to the south, east and north. Within this basin, the Ermua section was located at the base of the slope, whereas the Trabakua Pass section was deposited in a more basinward location.

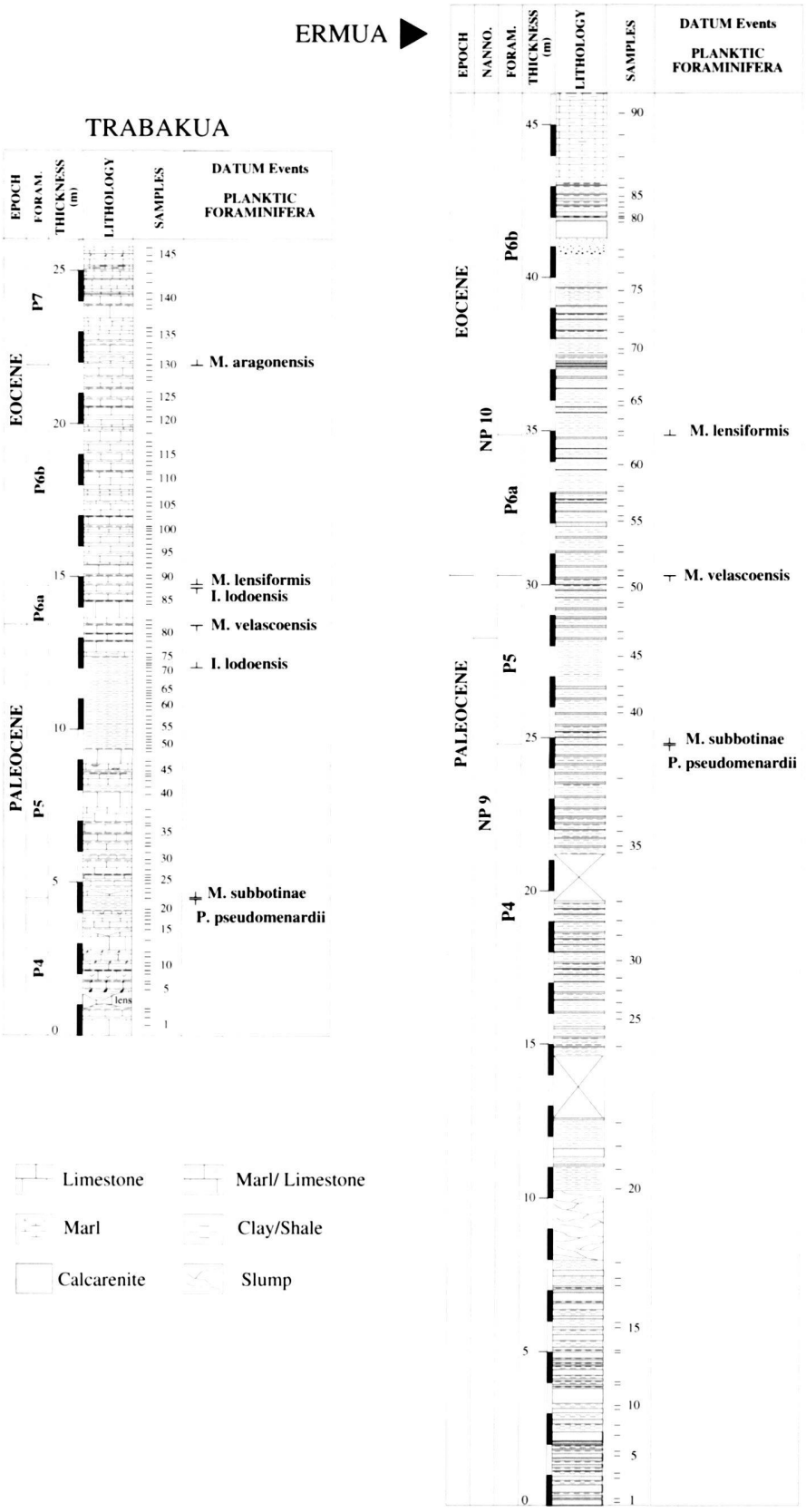

Fig. 2. Lithological description of the Trabakua Pass and the Ermua sections. Planktic foraminifera and calcareous nannoplankton zonation used in this study.

Lithology and sampling

The Trabakua section is about 26 m thick and spans the Paleocene-Eocene (P-E) transition (Fig.2). The lower part of the section (0 to 9.3 m) consists of alternating hemipelagic marls and limestones. The middle part (9.3 to 12.3 m) is composed of green laminated clays alternating with reddish clays and the upper part of the section (12.3 to 25.7 m) consists of alternating hemipelagic limestones and marl layers. This interval consists of more massive limestone and marl layers than the lower part of the section. We sampled the section at 10 to 20 cm intervals, except in the green/reddish clay layers where samples were collected at 5 to 10 cm intervals. A total of 146 samples were analyzed for this study.

The Ermua section is about 45 m thick and also spans the P-E transition (Fig. 2). This succession is mainly built up of turbidites grading upward from coarse grained sandy calcarenites into hemipelagic marls. The calcarenites are rich in quartz and other reworked detrital material. Limestones and marl layers are more massive in the uppermost three meters of the section. Samples in the marly layers were collected at 10 to 90 cm intervals. A total of 90 samples were analyzed for this study.

Methods

Foraminifera:

Sediments were soaked in water and washed through a 63 μm sieve. An ultrasonic bath was used to further clean the recovered foraminiferal tests. Washed residues were dried in an oven. Foraminifera were picked from the residues (>106 μm) for identification and biostratigraphic determinations.

Calcareous nannofossils:

Simple smearslides were prepared and studied with the light microscope at a magnification of 1000 x.

Mineralogical analyses:

X-Ray Diffraction (XRD) analyses of whole rock and clay mineral studies were conducted at the Geological Institute of the University of Neuchâtel, Switzerland, using a SCINTAG XRD 2000 Diffractometer. Whole rock samples were prepared following the method of Kübler (1987). For each rock sample, approximately 20 g were ground to obtain small rock chips (1 to 5 mm). Of these, 5 g were dried at a temperature of 60 °C and then ground again to a homogenous powder with particle size < 40 μm. 800 mg of this powder was compressed (20 bars) in a powder holder and analyzed by XRD. Whole rock composition was determined using external standards based on the methods described by Ferrero (1965, 1966), Klug & Alexander (1974), Kübler (1983), and Moore & Reynolds (1989).

Clay mineral analyses were based on the methods of Kübler (1987). Ground chips were mixed with de-ionized water (pH 7–8) and agitated. The carbonate fraction was removed with 10% HCl (1.25 N) at room temperature for 20 minutes or more until all the carbonate was dissolved. Ultrasonic disaggregation was performed for 3 minutes. The insoluble residue was washed and centrifuged (5–6 times) until a neutral suspension was obtained (pH 7–8). Separation of different grain size fractions (< 2 μm and 2–16 μm) was obtained by the timed settling method based on Stokes law. The selected fraction was then pipetted onto a glass plate and air-dried at room temperature. XRD analyses of oriented clay samples were made after air-drying in ethylen-glycol solvated conditions for the fraction < 2 μm. The intensities of selected XRD peaks characterizing each clay mineral (e.g., chlorite, mica, kaolinite, chlorite-smectite and illite-smectite mixed-layers) were measured for semi-quantitative estimates of the proportion of clay minerals present in the size-fractions < 2 μm and 2–16 μm. Clay minerals are therefore given in relative percent abundance without correction factors.

Stable isotopes:

Oxygen and carbon isotope analyses were conducted on bulk rock samples at the stable isotope laboratory at the University of Lausanne, Switzerland. Carbonate samples were prepared following the conventional procedure of McCrea (1950). CO_2 released from a 2 hour reaction between powdered bulk samples and 100% phosphoric acid at 50 °C was analyzed. The $\delta\ ^{13}C$ and the $\delta\ ^{18}O$ composition of the released CO_2 gas was measured on a Finnigan MAT 251 spectrometer. The results are reported in the usual per mil δ -notation relative to the PDB (Pee Dee Belemnite) international isotopic standard. In the isotope laboratory at the University of Lausanne, calibration to PDB is performed by Carrara marble versus NSB19 standard. Replicate analysis of selected samples showed a reproducibility of 0.05 per mil for $\delta\ ^{13}C$ and better than 0.1 per mil for $\delta\ ^{18}O$. (Bartolini et al. 1996)

Organic matter:

Organic carbon was analyzed using a CHN Carlo-Erba Elemental Analyzer NA 1108. This instrument analyzes total carbon, hydrogen and nitrogen in solid samples by flash combustion at 1020 °C. The sample was placed in a tin container and introduced into a combustion column reactor by means of an auto-sampler (Verardo et al. 1990). The combustion product, a mixture of CO_2, NO and H_2O, is transported through the combustion reactor by a mobile phase of helium into a second column. Due to their different velocities, N is first detected, followed by C and H. Total carbon was first measured on bulk samples (0.01–0.02 g). Total organic carbon (TOC) was determined after dissolving carbonate with hydrochloric acid (HCl 10%). TOC values were determined by comparing the values obtained from the analysis of the sample with the analysis of a suitable standard (Cyclohexanone–2,4 dinitrophenyl Hydra-

zone ($C_{12}H_{14}N_4O_4$)) and the use of a known reference k-factor (Erba, C., instruction manual 1990). Analytical precision is ± 0.003% of the measured value.

Granulometry:

Measurements have been carried out using a Galai CIS I laser system. This system is based on a rotating He-Ne laser, where the time it takes to pass over a particle is related to the particle diameter. The standard measuring range extends from 0.5 µm to 150 µm in steps of 0.5 µm (Jantschik et al. 1992).

Atomic absorption:

The presence of the elements Ca, Sr, Fe, Mn, Mg and K was determined with a Perkin-Elmer 5100 PC Atomic Absorption Spectrophotometer in the Laboratory of petrology and mineralogy at the Institute of Geology, University of Neuchâtel, Switzerland.

Results

Biostratigraphy

Foraminifera

Planktic and benthic foraminifera in both the Trabakua and Ermua sections are very poorly preserved, recrystallized and/or phosphatized though common at Trabakua, but rare at Ermua in most samples. In general, up to a dozen species can be identified per sample. This is generally enough to obtain biostratigraphic control, though placement of zonal boundaries may be tentative because of the rarity and poor preservation of index species.

Nevertheless, biostratigraphic determinations of this study are in relatively good agreement with earlier studies by Coccioni et al. (1994) and Orue-Etxebarria et al. (1996). The planktic foraminiferal zonation used in this study is the revised zonation of Berggren et al. (1995). For the Paleocene-Eocene interval, this zonal scheme differs from earlier zonations, where the original Zone P5 had been eliminated or effectively included in Zone P6a. Now, Zone P5 is used in a larger sense, including P5 and P6a of earlier publications. Thus this zonal name change will cause great confusion when sections are correlated with earlier published P-E studies where the benthic extinction event and carbon-13 shift is known to occur in Subzone P6a, which is now labelled Zone P5.

Zone P4: This zone is defined by the total range of *Planorotalites pseudomenardii.* At the Trabakua and Ermua sections this taxon disappears at 4.5 m and 25 m from the base respectively (Fig. 2). In both sections the faunal assemblages in this interval are dominated by subbotinids (e.g. *Subbotina triloculinoides, S.hornibrooki, S.velascoensis*) and conicate acarinids (e.g. *Acarinina subsphaerica, A.mckannai, A.nitida). Igorina pusilla, Planorotalites pseudoimitata, P. pseudomenardii* and *P. ehrenbergi* are generally present.

Morozovellids are extremely rare (single occurrence of *M. occlusa* and very rare *M. acuta*). In contrast, tropical assemblages of Zone P4 are dominated by discoidal morozovellids, including *M. occlusa* and *M. velascoensis* (Lu & Keller 1995a). The near absence of these tropical taxa in the Pyreneean sections indicates a relatively cool water environment as also suggested by the abundance of subbotinids.

Chiloguembelinids (e.g. *C. crinita, C. wilcoxensis* and *C. subcylindrica*) are present in the Ermua section in the uppermost part of Zone P4 (21.4 m) and continuing upwards into Zone P5 (29.5 m). The presence of these low oxygen tolerant taxa, as well as the generally dwarfed size of acarinids and subbotinids, particularly in the lower part of this interval, and the presence of low oxygen tolerant benthic foraminifera (bolivinids and buliminids), suggest that low oxygen conditions prevailed at this time. No chiloguembelinids were observed in the Trabakua section in Zone P4, however, many samples were barren due to dissolution in the upper part of Zone P4. The basal part of the Ermua section investigated contains only rare subbotinids and small acarinids. No *P. pseudomenardii* were found, though Orue-Etxebarria et al. (1996) noted the presence of this index species in this interval. We therefore tentatively identify the basal part as Zone P4.

Zone P5: This zone marks the biostratigraphic interval between the last occurrence of *Planorotalites pseudomenardii* and the last occurrence of *Morozovella velascoensis.* Note that this zonal re-definition by Berggren et al. (1995) includes the formerly known Zone P5 which marked the interval between the last occurrence of *P. pseudomenardii* and the first occurrence of *M. subbotinae* (Berggren & Miller 1988), and the formerly known Zone P6a, which marked the interval between the first occurrence of *M. subbotinae* and the last occurrence of *M. velascoensis.* The benthic extinction event, rapid faunal turnover and increased diversity in planktic foraminifera, and the carbon-13 isotopic excursion occur in the upper part of this interval worldwide within a carbonate-poor clay layer (e.g. Canudo et al. 1995; Lu et al. 1995; Lu & Keller 1995a, 1995b; Schmitz et al. 1995; Ortiz 1996; Thomas & Shackleton 1996).

At Trabakua and Ermua, the base of Zone P5 is at 4.5 m and 25 m respectively, marked by the last appearance of *P. pseudomenardii* and the first appearance of *M. subbotinae* within the same sample (Fig. 2). The top of this zone can only be tentatively identified in these sections because many samples have only rare foraminifera due to dissolution. This is particularly the case in the clay layer at Trabakua (9.3 to 12.3 m), and intermittently in the Ermua section. At Trabakua, the last *Morozovella velascoensis* was observed at 13.5 m which is about 1m above the top of the clay layer. At DSDP Site 577, Lu & Keller (1995a) noted that the short ranging species *Igorina lodoensis* marks the interval equivalent to Subzone P6a. *Igorina lodoensis* first appears at Trabakua near the top of the clay layer (12 m). This suggests that the Zone P5/P6a bound-

ary may be lower. At Ermua, *M. velascoensis* disappears at 30.3 m; *Igorina lodoensis* was not observed. Zone P5 assemblages at Trabakua and Ermua are dominated by acarininids (*A. mckannai, A. nitida, A. densa, A. pseudotopilensis*) and few morozovellids (*M. aequa, M. occlusa*).

Zone P6a: This zone is defined by the stratigraphic interval from the last *M. velascoensis* to the first appearance of *M. formosa* and/or *M. lensiformis*. *Morozovella lensiformis* is constantly present in the Trabakua and Ermua sections and we base the top of P6a at the first appearance of this taxon. At Trabakua, *M. lensiformis* appears at 14.5 m and only one meter above the last *M. velascoensis* (Fig. 2). This suggests either diachronous species occurrences, or a very condensed interval above the clay layer. There is no evidence for the latter in these limestone/marl layers, though a short hiatus could be present. At Ermua the first *M. lensiformis* was observed at 35 m and hence indicates that Zone P6a spans 5 m (Fig. 2). In both sections, Zone P6a is marked by higher planktic foraminiferal diversity than either above or below. This was also observed at other sections in Spain and elsewhere (Canudo et al. 1995; Lu & Keller 1995a, 1995b; Lu et al. 1996). The assemblages in this interval contain more morozovellids (*M. aequa, M. quetra, M. subbotinae, M. marginodentata*). In addition, rounded acarininids dominate (*A. pseudotopilensis, A. soldadoensis, A. praepentacamerata*) and replace the earlier conicate acarininid assemblage (*A. nitida, A. subsphaerica, A. mckannai*) as also observed in sections elsewhere (see Lu & Keller 1995a, 1995b). This major faunal turnover between P5 and P6a correlates with the maximum warming following the benthic extinction event and carbon-13 shift in other Tethyan (e.g. Caravaca, Zumaya, Allamedilla) in Spain (Canudo et al. 1995) and Negev sections (Lu et al. 1996).

Zone P6b: This zone spans the interval from the first appearance of *M. lensiformis* to the first appearance of *M. aragonensis*. At Trabakua, *M. aragonensis* appears at 22 m and the zone spans 7.5 m (14.5–22 m) (Fig. 2). At Ermua, *M. aragonensis* was not encountered in the examined interval; Zone P6b thus spans from 35 m to the top of the section (Fig. 2). The faunal assemblages in this interval are diverse. Rounded acarininids still dominate, though angulate morphotypes appear (*A. nicoli, A. densa*), and morozovellids are more common.

Zone P7: The base of Zone P7 is defined by the first appearance of *M. aragonensis*. This zone was only sampled at Trabakua where *M. aragonensis* was observed at 22 m; thus the upper most 4 m of the section belong to Zone P7. The assemblage is dominated by large rounded and angulate acarininids (e.g. *A. densa, A. triplex, A. primitiva, A. appressocamerata, A. soldadoensis, A. pseudotopilensis*) and morozovellids (*M. aragonensis, M. lensiformis*).

Calcareous nannofossils

Only the calcareous nannofossils of the Ermua section were studied in detail. While some samples were barren of any calcareous nannofossils, they are very rare to common in others. The preservation is usually poor, sometimes poor to moderate.

Zones NP9 and NP10: *Discoaster multiradiatus* is present from the lowermost studied sample on upwards thus indicating the presence of NP9, the *Discoaster multiradiatus* Zone of Martini (1971) in the lower part of the section (Tab. 1). A subdivision of NP9 has been suggested by various authors based on the first occurrence (FO) of *Campylosphaera dela* or the FO of *Rhomboaster sp.* This subdivision can only be applied in assemblages with a better preservation than the one observed in the present material.

The base of NP10, the *Rhomboaster bramlettei* Zone of Martini (1971), is defined by the FO of the namegiving species. In recent papers there has been an as of yet unresolved controversy about the correct determination and generic assignment – *Rhomboaster* or *Tribrachiatus* – of this species.

Representatives of *Rhomboaster/Tribrachiatus* were only found over a short part of the section (Tab. 1) and include *Rhomboaster* sp., *R. cuspis, R. bramlettei* and *R. spineus*. *Fasciculithus sidereus*, a species which has its last occurrence (LO) in the basal part of NP10 according to Bybell & Self-Trail (1995), was found by these authors and also at Ermua to overlap with *Rhomboaster bramlettei* and *R. spineus*. Bybell & Self-Trail (1995) have lumped together *R. cuspis* and other species of *Rhomboaster* into an enlarged *R. bramlettei*, thus lowering the base of NP10 below the level where authors separating *R. cuspis* and *R. bramlettei* would place it. *R. cuspis* usually appears before *R. bramlettei*. Wei & Zhong (1996) included some forms previously assigned to *R. bramlettei, R. calcitrapa, R. spineus* and *R. bitrifida* into the stratigraphically oldest species of the genus, *R. cuspis*. They assigned the remaining bramlettei to Tribrachiatus. Angori & Monechi (1996) included *R. cuspis, R. calcitrapa* and *R. bitrifida* in *R. bramlettei*, while retaining *R. spineus*. They then went on to register *R. bramlettei* with "short arms" (oldest), "long arms" and "var. T" (youngest), the latter appearing still before *R. contortus*. In conclusion, the lower boundary of NP10 is presently applied differently by different authors according to their concept of the defining species *R. bramlettei*.

Orue-Etxebarria et al. (1996) did not report *F. sidereus* from the Ermua section, but found other fasciculiths to overlap with *R. spineus* and *R. bramlettei* (their *Tribrachiatus nunnii*). The NP9/NP10 boundary is in this study placed at the first occurrence of *R. bramlettei*, following the original definition of the zonal boundary.

Aubry (1996) has subdivided NP10 based on the evolution of *Rhomboaster/Tribrachiatus*. This seems to be not applicable in the present section due to the scarcity or absence of *Rhomboaster* and *Tribrachiatus* respectively in the upper part of the section. Also the subdivision based on the FO of *Discoaster diastypus* could not be applied, since this species was not found in the scarce and poorly preserved assemblages available from that part of the section. It was, however, found by Orue-Etxe-

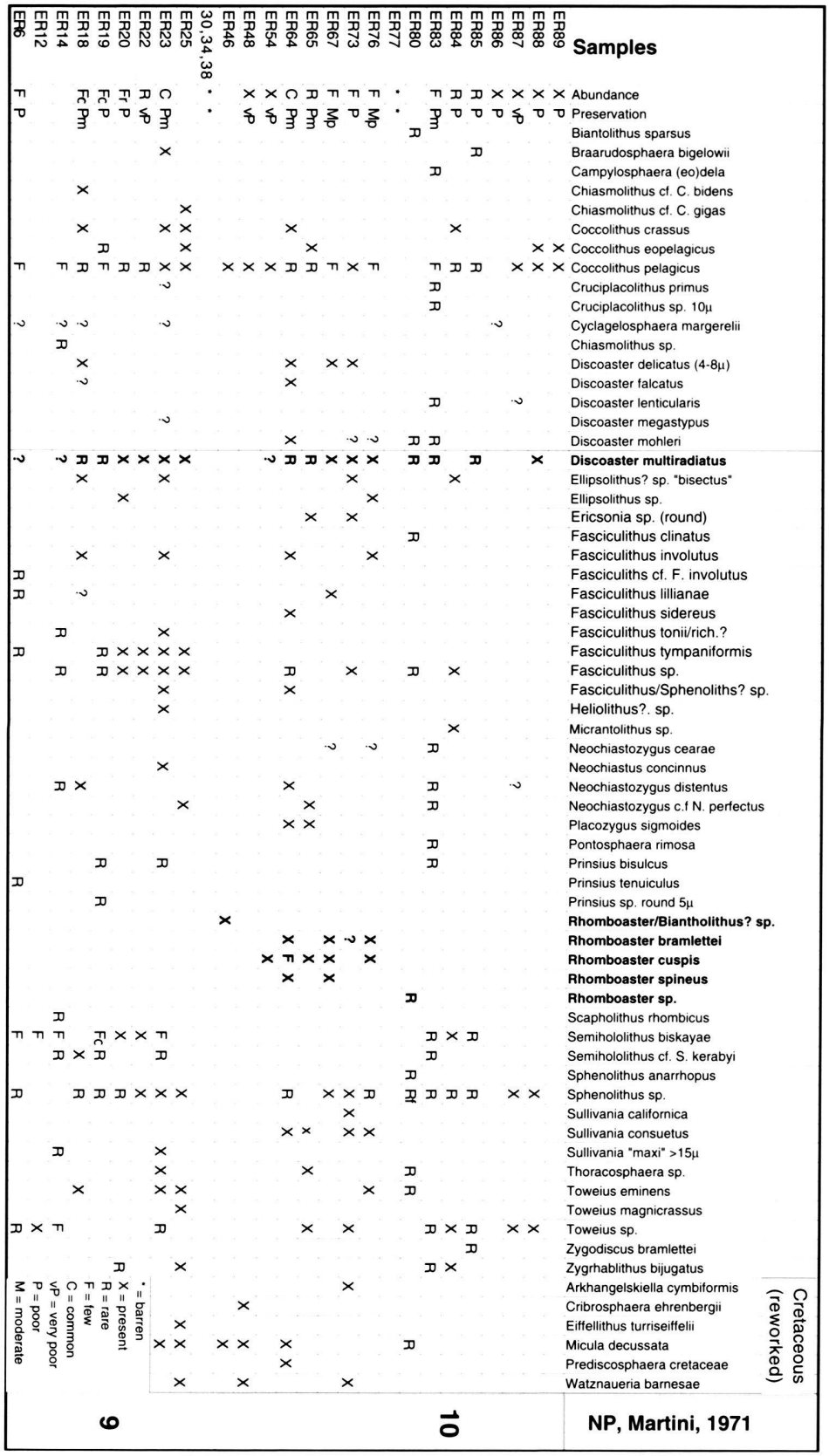

Tab. 1. Ermua section: Relative abundance, degree of preservation of calcareous nannofossils.

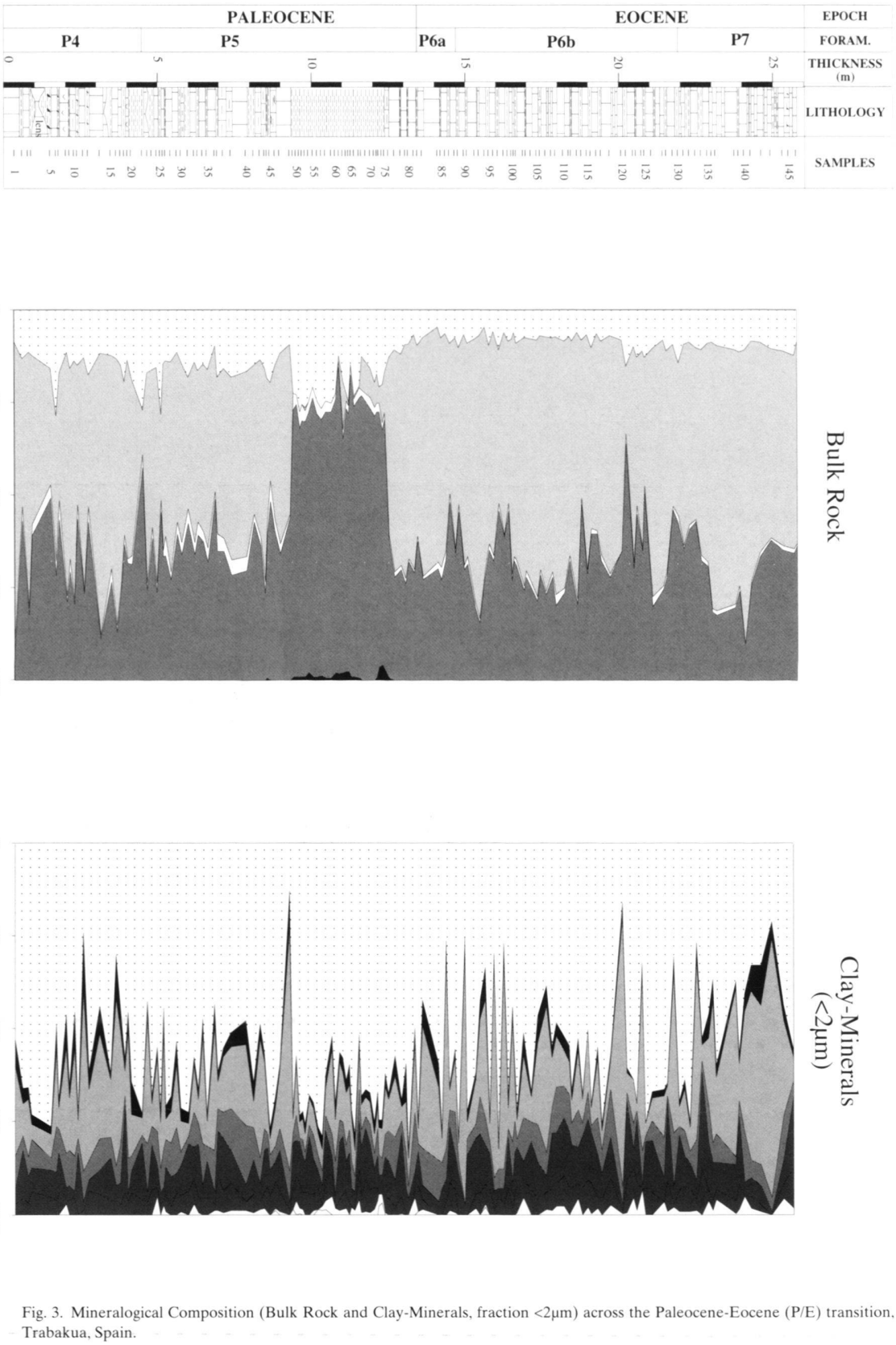

Fig. 3. Mineralogical Composition (Bulk Rock and Clay-Minerals, fraction <2µm) across the Paleocene-Eocene (P/E) transition, Trabakua, Spain.

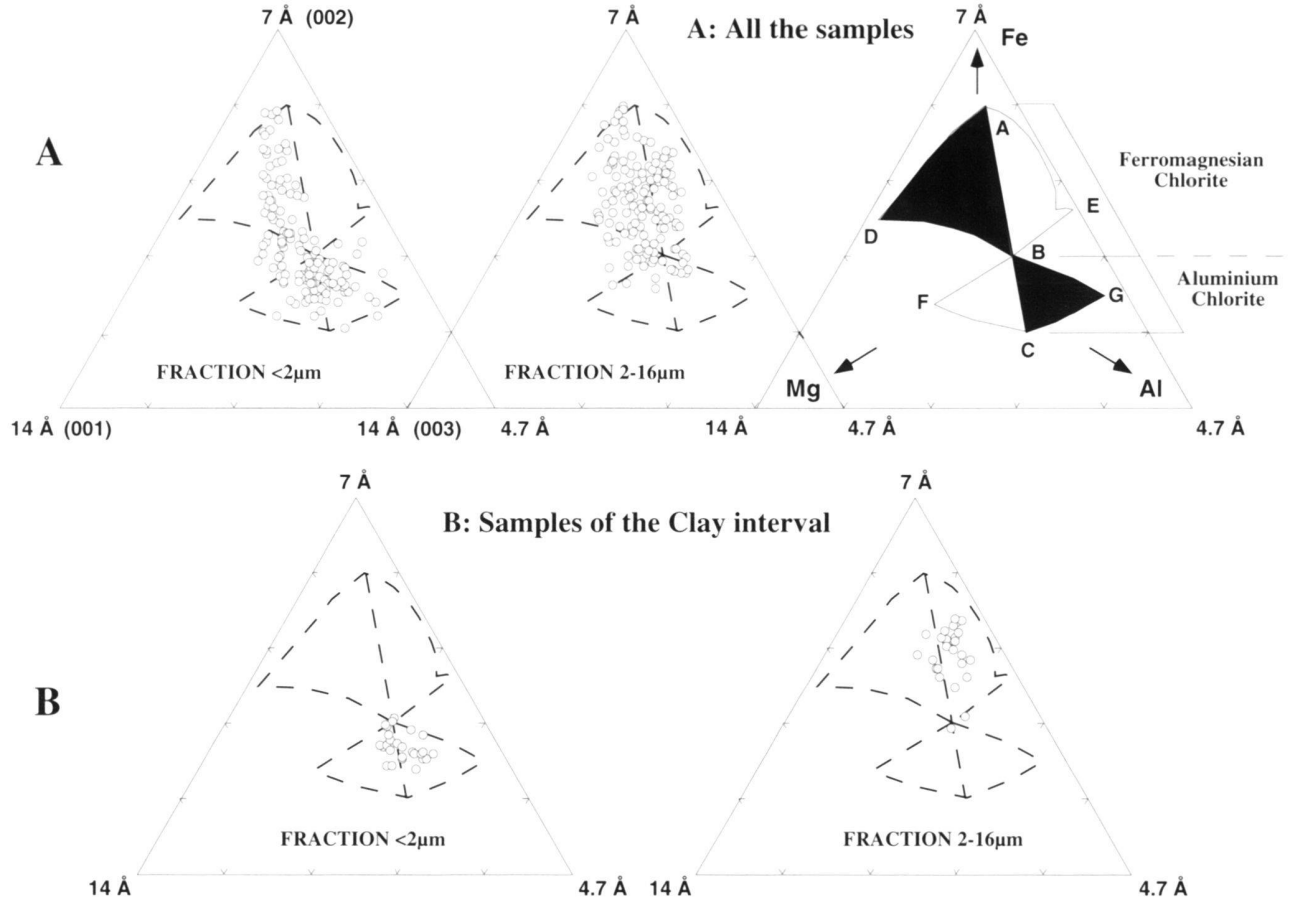

Ternary diagram 001 (14Å), 002 (7Å) and 003 (4.7Å)

Fig. 4. Chemical nature of chlorite, Trabakua, Spain.
Ternary diagramm after Oinuma, Shimoda & Sudo, 1972.
Field ABDE indicates ferromagnesian chlorites. Field ABD = Iron excess in silicate layers. Field ABE = Iron excess in hydroxyl layers. Field BFCG indicates aluminium chlorites. Field BCG = Aluminium excess in silicate layers. Field BCF = aluminium excess in hydroxyl layers.

barria et al. (1996) who had samples also from higher up in the section.

Reworked Cretaceous coccoliths are very rare and include only relatively solution resistant forms (Tab. 1).

Mineralogy

Trabakua Pass section

Bulk rock analyses of the Trabakua Pass section indicate that calcite is the dominant component in the limestone-marl sequence between 0 to 9.3 m, with a mean value of 48% (Fig. 3). In the upper more massive limestone-marl sequence, between 12.3 and 25.75 m, calcite averages 58%. The 3 m thick interval of green/reddish clay (9.3 to 12.3 m) is marked by an abrupt decrease in calcite to 2%. The dramatic decrease in calcite coincides with a corresponding increase in phyllosilicates, from an average of 32–34% above and below the clay layer to an average of 75% and a maximum of 83%.

Detrital minerals are a minor component of the sediments and include primarily quartz, some plagioclase and K-feldspar. Quartz averages 17% below the clay layer and 11% above it. Within the clay layer, quartz content increases to 25% in the lower half and decreases to an average of 17% in the upper

half of the clay interval. Plagioclase and K-feldspar reach 3% and 1% respectively in this interval. Hematite, a strong coloring agent, has been observed in the reddish layers of the clay interval and may be responsible for the color. Under oxidizing conditions, this mineral forms at neutral to high pH (Velde 1995).

These mineralogical changes across the clay layer probably indicate a decrease in the primary productivity of carbonates and variations in sediment sources and/or oceanic currents.

The composition of the clay mineral association (< 2 μm fraction) varies strongly throughout the section with mica as the dominant mineral, averaging 55% to 57%. In the clay layer, mica increases to 67% (Fig. 3). Chlorite is present throughout the section with an average of 19%, but decreases in the clay interval to 9%. Kaolinite averages 3.5% (0 to 11%) and is a minor component. Mixed-layer illite-smectite (IS) and chlorite-smectite (CS) contents have mean values of 14% and 7% respectively. Smectite and rectorite contents are very low (< 1%). The clay mineral distributions of the clay interval are thus not significantly distinct from those in the rest of the section. Only a slight increase in mica and decrease in chlorite can be observed.

The chemical composition of chlorite is shown in ternary diagrams (Fig. 4 after Oinuma et al. 1972) where the poles 14Å, 7Å and 4.7Å indicate magnesian, iron and aluminium respectively. The chemical nature of chlorite within the clay interval depends on the grain size. Chlorite is aluminous in the fraction < 2 μm and ferromagnesian in the fraction 2–16 μm. The ferromagnesian chlorite in the fraction < 2 μm is restricted to the field ABD which shows an iron excess in the chlorite's silicate layers. Two generations of chlorite can be observed, a ferromagnesian and an aluminous generation which have two origins, the first more important one detrital and the second one diagenetic. Magnesium and iron released during the transformation of smectite to illite could favor the formation of diagenetic chlorite (Hower et al. 1976). Kaolinite is also a potential source of Al and Si for aluminous chlorite formation during burial diagenesis (e.g. Muffler & White 1969; Perry & Hower 1970; Boles & Francks 1979).

Clay minerals generally reflect climatic conditions. For example, high abundance of kaolinite indicates warm, or humid climates, well-drained continental areas with high precipitation and accelerated leaching of parent rocks (Millot 1970; Chamley 1989; Weaver 1989). Increased chlorite and mica contents indicate cold or arid (desert) conditions with active mechanical erosion (Millot 1970). However, post-depositional diagenetic alteration may obliterate or obscure the climate signal.

For example in the Trabakua section, the near absence of smectite and the low kaolinite content (< 4%) are not linked to climatic conditions, nor to a particular depositional environment, but to a diagenetic overprint. This is suggested by the presence of diagenetic chlorite, mixed-layers chlorite/smectite and illite-smectite, the near absence of smectite, rectorite and kaolinite. The clay mineral contents of the Trabakua Pass sediments thus indicate deep burial diagenesis that corresponds approximately to the end of zone 3 of Kübler et al. (1979). In contrast, the Zumaya section, located in the Basque basin about 30 kilometers to the north-east, in a similar sedimentary environment, has retained the climatic signals. In this section, during the Paleocene-Eocene transition, the clay mineral composition consists of mica, mixed-layers illite-smectite, chlorite and large amounts of smectite and kaolinite (Adatte et al. 1995). The presence of smectite and the increase in chlorite and mica during the P-E transition suggest arid conditions in the adjacent continental areas where kaolinite is absent. Kaolinite would probably have been transported from lower latitude by oceanic currents.

Ermua section

Bulk rock composition of the Ermua section shows high variability (Fig. 5). In the lower part of the section (0 to 16 m) calcite is the dominant component in the hemipelagic marls and the carbonate turbidites with a mean value of 42% and 31% respectively. In the upper more massive carbonate turbidite sequence between 41 to 46 m, calcite averages 49%. Between these lithologies (16 to 41 m), calcite content decreases drastically with a mean value of 4% in hemipelagic marls and 21% in calcarenites. This decrease coincides with an increase in phyllosilicates in the hemipelagic marls, from an average of 36% below the middle part of the section (16 to 41 m) to an average of 67%. In the calcarenites, the phyllosilicates increase also from a mean value of 21% to 57%. In the upper massive limestone, the phyllosilicate content reaches an average of 35%. Detrital minerals are a minor component of the sediments and include primarily quartz, some plagioclase and K-feldspar. Below 16 m, quartz averages in the hemipelagic marls and in the calcarenites 17% and 36% respectively. Above 41 m quartz reaches a mean value of 11%. Between 16 m and 41 m, the proportion of quartz in the calcarenites decreases to a mean value of 17% and increases in the hemipelagic marls to an average of 25%. Plagioclase and K-feldspar are minor throughout the section with a mean value < 6% and < 1% respectively. Pyrite, goethite and apatite (phosphate) have been observed in the sandstones between 25 m and 39 m indicating a low oxygen environmental deposit.

Clay mineral contents also are variable throughout the section. In the lower part of the section (between 0 and 16 m) (Fig. 5) mica is the dominant mineral averaging 63 and 57% in hemipelagic marls and in calcarenites respectively. In the middle part (16–41 m) mica decreases with a mean value of 27% in calcarenites and 51% in marls. In the upper more massive limestones (41 to 46 m) mica increases to an average of 43%. The decrease in mica coincides with an increase in chlorite

Fig. 5. Mineralogical composition (Bulk Rock and Clay Minerals, fraction < 2 μm), Ermua, Spain.

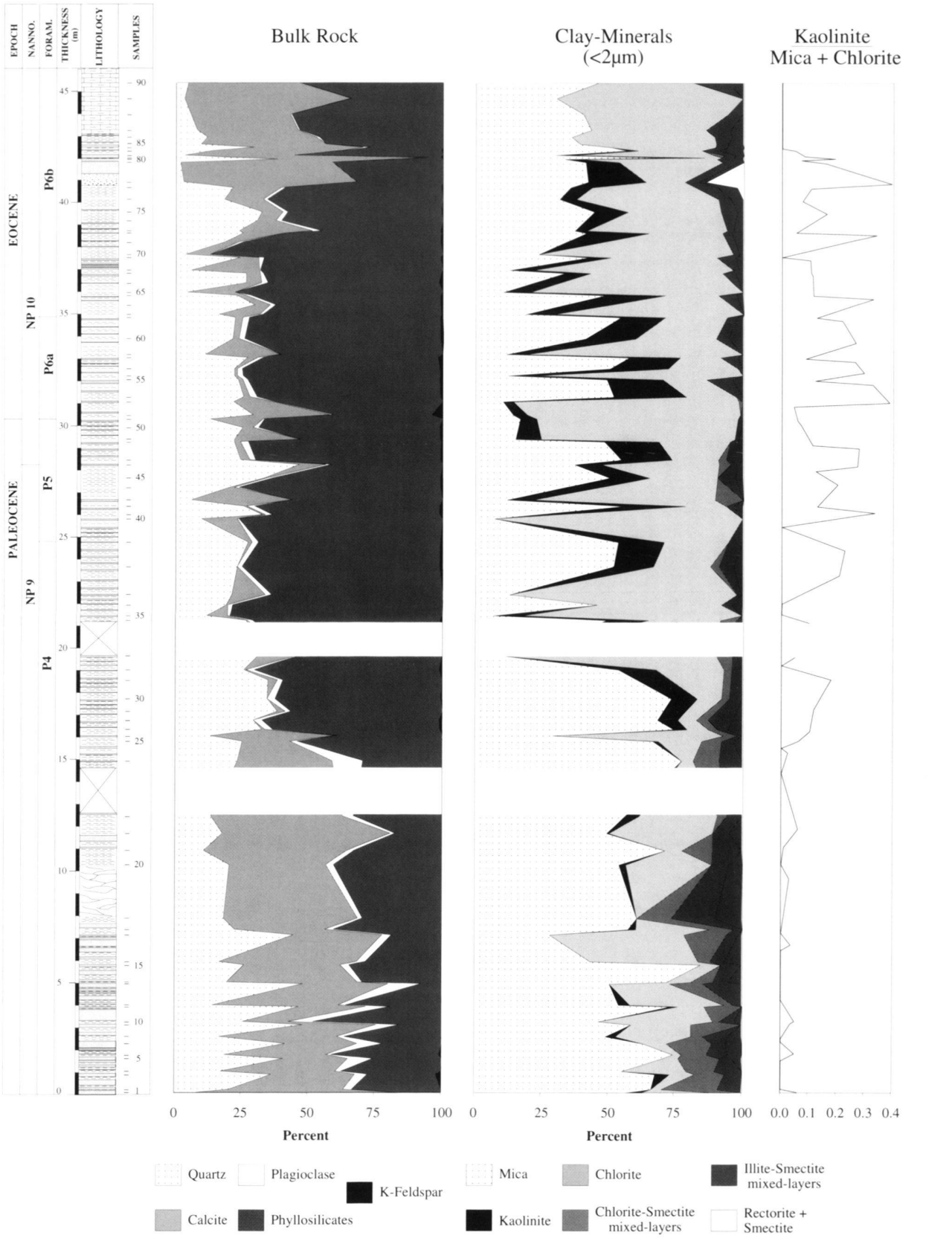
EPOCH
NANNO.
FORAM.
THICKNESS (m)
LITHOLOGY
SAMPLES
EOCENE
PALEOCENE
NP 10
NP 9
P6b
P6a
P5
P4
Bulk Rock
Clay-Minerals (<2µm)
Kaolinite Mica + Chlorite
Percent
Percent
Quartz
Plagioclase
K-Feldspar
Calcite
Phyllosilicates
Mica
Chlorite
Illite-Smectite mixed-layers
Kaolinite
Chlorite-Smectite mixed-layers
Rectorite + Smectite

from an average of 17% to 74% in the calcarenites. In the hemipelagic marls, chlorite increases only from 22 to 26%. In the upper limestones (41 to 46 m), chlorite reaches a mean value of 40%. Kaolinite is a minor component in the sediments with a mean value < 2% between 0 and 16 m, an average of 14% and 6% in hemipelagic marls and calcarenites respectively between 16 m and 41 m, and a mean value of 3% in the last 5 meters. Mixed-layer illite-smectite (IS) contents have a mean value of 10% in the hemipelagic marls throughout the section. In the calcarenites (0 to 16 m), the IS content attains an average of 6% and decreases to 2% between 16 m and 41 m. Mixed-layer chlorite-smectite (CS) shows a mean value of 17% in the calcarenites and 7% in the hemipelagic marls between 0 and 16 m. In the middle part the CS content decreases to an average of 1% in the two lithologies. The upper, more calcareous sediments are marked by the absence of CS and by an IS content with a mean value of 9%.

Major changes were observed in the interval between 16 m and 41 m which is marked in the hemipelagic marls by an increase in kaolinite and chlorite and an important decrease in mica. In the calcarenites of this interval, mica and IS decrease whereas chlorite and kaolinite increase. The relatively high amount of kaolinite in the interval between 16 and 43 m suggests that the sediments are less affected by burial diagenesis and/or tectonic activity than in the Trabakua Pass section. In the Ermua section clay minerals retain therefore climatic signals. Chlorite and mica indicate cold or arid (desert) conditions with active mechanical erosion. In contrast kaolinite typically develops in tropical soils on poorly drained surfaces with high precipitation. The joint increase of chlorite and kaolinite between 16 m and 41 m and the higher content of kaolinite in hemipelagic marls compared to calcarenites imply different sources characterized by opposite climatic conditions and different ways of transport. Therefore, these mixed associations suggest that arid conditions prevailed in the adjacent coastal area whereas kaolinite was brought from lower latitudes by oceanic currents.

Stable isotopes

Trabakua Pass section

Bulk rock carbonate was analyzed for $\delta^{13}C$ and $\delta^{18}O$ isotopes in the interval between 3 m and 20 m at the Trabakua Pass section (Fig. 6 and Tab. 2).

In sediments of the Trabakua section, carbonates are affected by recrystallization/diagenesis which obscure, alter or obliterate the $\delta^{18}O$ signals, but not the $\delta^{13}C$ signals. Early diagenetic alteration of carbonate $\delta^{18}O$ and $\delta^{13}C$ of the K/T and early Paleocene sediments in the Negev of Israel has been studied by Magaritz et al. (1992). By comparing the isotopic values from whole-rock and two fine fractions, these authors concluded that $\delta^{13}C$ signals were not significantly altered, whereas $\delta^{18}O$ signals were strongly affected by meteoric water during early diagenesis. Dissolution and recrystallization often do not significantly influence the magnitude of the $\delta^{13}C$ shift in deep sea sequences whereas the primary oxygen isotope is overprinted by diagenesis (Veizer 1983). $\delta^{18}O$ values are very negative (–3.8 to –4.9 ‰) and constant throughout the Trabakua section, thus indicating secondary recrystallization or alteration by meteoric water.

Tab. 2. Trabakua section: Analyses of stable isotopes ($\delta^{13}C$ and $\delta^{18}O$), total carbon and calcite.

Samples	δ 13 C	δ 18 O	Total Carbon	Calcite
	(‰)		(%)	
TB14	2,54	-4,45		75,98
TB19	2,52	-4,62	7,50	53,90
TB28	2,00	-4,63	7,12	56,49
TB34	1,68	-4,67	6,39	45,36
TB38	1,88	-4,73	6,10	45,95
TB40	1,69	-4,72	6,28	49,99
TB41	1,46	-4,99	4,99	40,08
TB42	1,87	-3,92	6,63	48,12
TB43	1,42	-4,80	5,87	57,61
TB44	1,06	-4,84	4,32	39,03
TB45	0,71	-4,66	2,77	26,32
TB46	0,92	-4,58	5,06	41,28
TB62	-0,59	-4,57	0,70	12,99
TB72	-1,14	-4,20	1,05	8,04
TB74	-1,42	-4,56	1,04	10,17
TB75	-1,00	-4,62	1,36	10,89
TB76	0,32	-4,75	6,01	47,87
TB77	0,85	-4,67	8,13	60,09
TB78	0,67	-4,45	6,74	56,99
TB79	1,03	-4,66	8,66	63,08
TB80	0,69	-4,40	7,17	57,76
TB81	1,04	-4,63	9,45	63,50
TB85	0,97	-4,48	7,72	62,00
TB90	1,27	-4,65		62,37
TB95	0,84	-4,47	6,07	57,37

Below the clay layer, between 3 m to 9.3 m, $\delta^{13}C$ values gradually decrease from 2.5 to 0.95 ‰. A similar decrease preceding the clay layer was also observed at Alamedilla, Spain (Lu et al. 1996, Fig. 12). Within the clay layer $\delta^{13}C$ values decrease by 1.4‰ and reach minimum values (– 1.4‰) between 12.15 and 12.45 m. The absence of $\delta^{13}C$ data in the lower part of the clay layer is due to the very low carbonate content (<2%). Between 12.45 m and 12.5 m, $\delta^{13}C$ values rapidly increase by 1.3‰. Above this interval (12.65 m), bulk $\delta^{13}C$ values gradually increase (0.8 to 1.2‰).

Bulk $\delta^{13}C$ values correlate well with the carbonate curve (Fig. 6). In both datasets, there is a gradual decrease below the clay layer, an abrupt decrease within, and a gradual increase above it.

Fig. 6. Stable isotopic changes ($\delta^{13}C$ and $\delta^{18}O$) across the Paleocene-Eocene transition, correlated with Organic Matter, Total Carbon and Calcite variations, Trabakua, Spain.

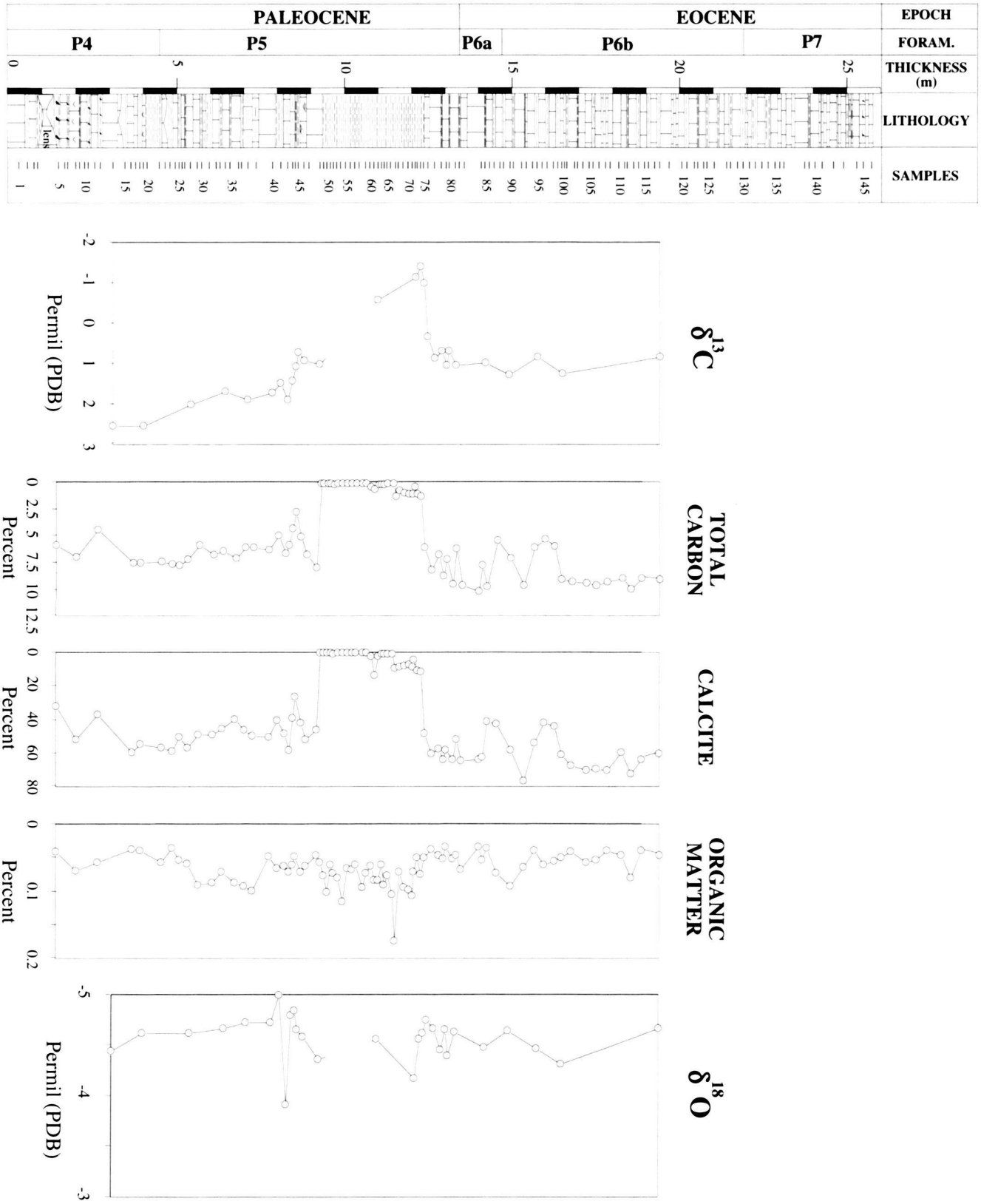
PALEOCENE
EOCENE
EPOCH
P4
P5
P6a
P6b
P7
FORAM.
THICKNESS (m)
LITHOLOGY
lens
SAMPLES
Permil (PDB)
δ13C
TOTAL CARBON
Percent
CALCITE
ORGANIC MATTER
δ18O

Ermua section

Bulk rock carbonate was analyzed for $\delta^{13}C$ and $\delta^{18}O$ isotopes in hemipelagic marls between 0.2 m and 44 m in the Ermua section (Fig. 7 and Tab. 3) in order to determine the presence of a $\delta^{13}C$ shift correlative with the clay layer at Trabakua. Unfortunately, relatively few samples are rich in calcite and hence isotopic data are of low sample resolution and low reliability in some samples. However, the following trends can be tentatively determined. Between 0 and 15 m where calcite averages 40% $\delta^{13}C$ values gradually decrease from 1.4 to 0.6‰. Between 16 and 41 m, where calcite is nearly zero (< 2%) $\delta^{13}C$ values are very low with an average of – 2.6‰. These very low values of $\delta^{13}C$ may be explained by the presence of lithologies very poor in carbonates but enriched in organic matter. In the limestone interval at the top of the section $\delta^{13}C$ values increase from – 0.6 to 0.9‰.

At Ermua, the negative $\delta^{13}C$ excursion occurs in the middle part of the Zone P4 contrary to the carbon–13 isotopic excursion in the upper part of P5 in the Trabakua section within a carbonate-poor clay layer. The two negative $\delta^{13}C$ excursion are thus not correlatable and cannot be used as chronostratigraphic markers.

As in the Trabakua section, oxygen isotope values (–4.6 to –5.7‰) reflect diagenetic alteration rather than original paleotemperatures.

Tab. 3. Ermua section: Analyses of stable isotopes ($\delta^{13}C$ and $\delta^{18}O$), total carbon, organic matter and calcite.

Samples	δ 13 C	δ 18 O	Total Carbon	Organic Matter	Calcite
	(‰)	(‰)	(%)	(%)	(%)
ER2	1,45	-4,36	5,06	0,20	43,09
ER6	1,09	-4,30	4,43	0,22	38,07
ER14	1,18	-4,57	5,80	0,12	49,16
ER19	0,89	-4,54			50,24
ER20	0,78	-4,68	4,01	0,14	36,23
ER22	0,70	-4,50	7,19	0,11	62,88
ER23	0,60	-4,73			49,53
ER25	-2,82	-5,39	2,46	0,11	17,91
ER40	-2,58	-5,01	6,79	0,19	13,52
ER49	-2,67	-5,11	6,14	0,11	24,49
ER65	-2,06	-5,09	9,81	0,14	18,23
ER76	-2,43	-5,13			14,54
ER77	-2,94	-5,66	2,36	0,20	18,39
ER79	0,81	-4,75	11,65	0,06	57,08
ER84	-0,64	-5,59			40,77
ER85	0,16	-4,57	8,10	0,08	47,16
ER86	0,51	-4,60			40,90
ER87	0,63	-4,87	10,44	0,10	38,21
ER88	0,86	-4,32			37,45

Organic matter

Trabakua sediments are extremely poor in organic matter (<0.10%): below 0.1% values are considered background noise (Fig. 6). Only one sample within the clay layer reaches 0.197%. Ermua sediments have a relatively higher organic content (Fig. 8), varying between 0.1 to 0.5%. In the hemipelagic marls between 20 m and 40 m organic matter increases from an average of 0.15% to 0.25% whereas in the calcarenites it attains a mean value of 0.1%.

Oxygenation at the sea floor is controlled by the input of organic matter (e.g. Calvert 1987), oxygen content of bottom water, and circulation intensity. The oxygen depletion results from oxidation of organic matter which sinks through the water column, or is transported laterally (Wetzel 1991). An oxygen-depleted environment favours the formation of reduced minerals like pyrite. The absence of organic matter at Trabakua prevents the development of reducing conditions and favours the formation of iron oxides like hematite, a mineral observed in the clay layer. In the Ermua section the presence of organic matter and of pyrite seem to indicate a more reducing environment than at Trabakua.

Grain size

Grain size analyses in the Trabakua Pass section indicate that an average of 44% of the grains are in the < 4 μm size fraction which includes < 1 μm, 1–2 μm and 2–4 μm size fractions (Fig. 8). However, in the clay interval an average of 52% is attained in the < 4 μm fraction. The larger fraction 4–8 μm averages 38% throughout the section. The coarser grain fractions (between 8 and 32 μm) average 16% between 0 and 9.25 m and 18% in the interval between 12.45 m and 25.7 m. The coarse fraction decreases to an average of 10% in the clay interval. The decrease in the grain size in the clay interval suggests changes in ocean currents and/or reduction in the intensity of atmospheric circulation.

Geochemistry

Trabakua Pass

Significant changes occur in the clay layer of the Trabakua Pass section in all major components (Fig. 9). For example, calcium averages a mean value of 23% and 27% below and above the clay interval respectively, but decreases to 3% within the clay layer (9.3 to 12.3 m). Strontium averages 0.05% except in the clay layer where values decrease to 0.002%. Manganese averages 0.09% above and below the clay layer, but

Fig. 7. Stable isotopic changes ($\delta^{13}C$ and $\delta^{18}O$) across the Paleocene-Eocene transition, correlated with Organic Matter, Total Carbon variations, Ermua, Spain.

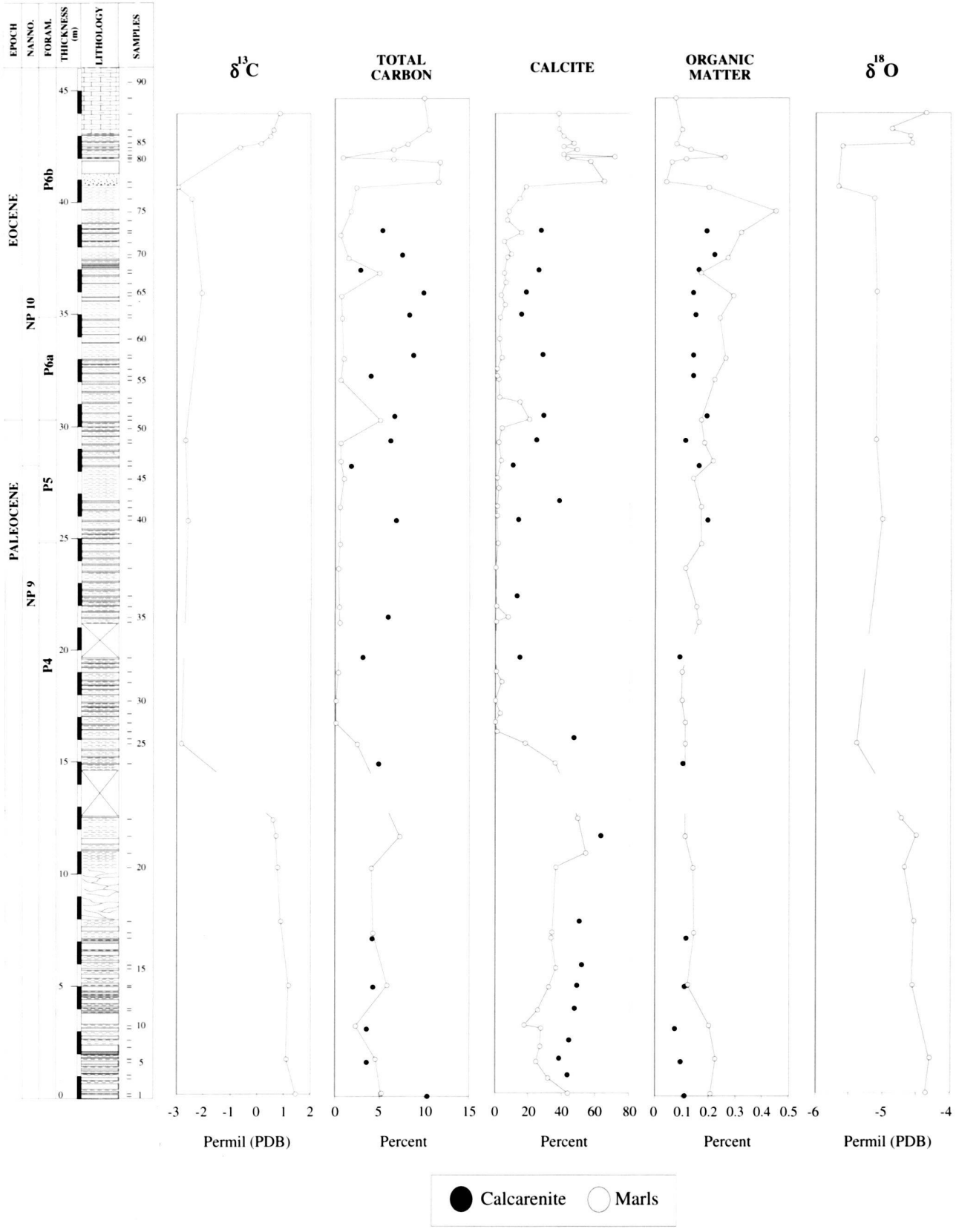
EPOCH
NANNO.
FORAM.
THICKNESS (m)
LITHOLOGY
SAMPLES
EOCENE
PALEOCENE
NP 10
NP 9
P6b
P6a
P5
P4
δ13C
TOTAL CARBON
CALCITE
ORGANIC MATTER
δ18O
Permil (PDB)
Percent
Percent
Percent
Permil (PDB)
Calcarenite
Marls

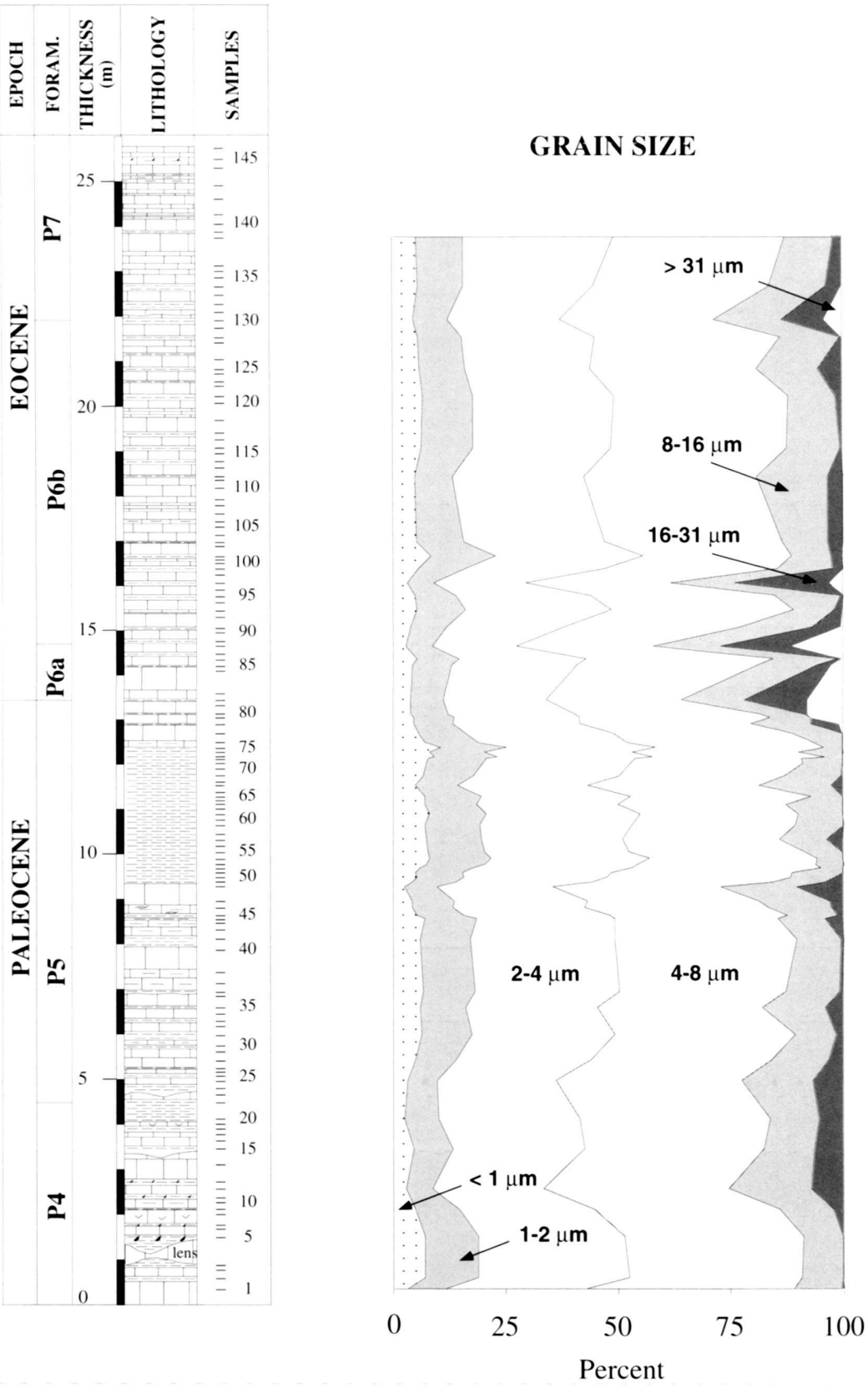
EPOCH
FORAM.
THICKNESS (m)
LITHOLOGY
SAMPLES
EOCENE
PALEOCENE
P7
P6b
P6a
P5
P4
25
20
15
10
5
0
145
140
135
130
125
120
115
110
105
100
95
90
85
80
75
70
65
60
55
50
45
40
35
30
25
20
15
10
5
1
lens
GRAIN SIZE
> 31 μm
8-16 μm
16-31 μm
2-4 μm
4-8 μm
< 1 μm
1-2 μm
0
25
50
75
100
Percent

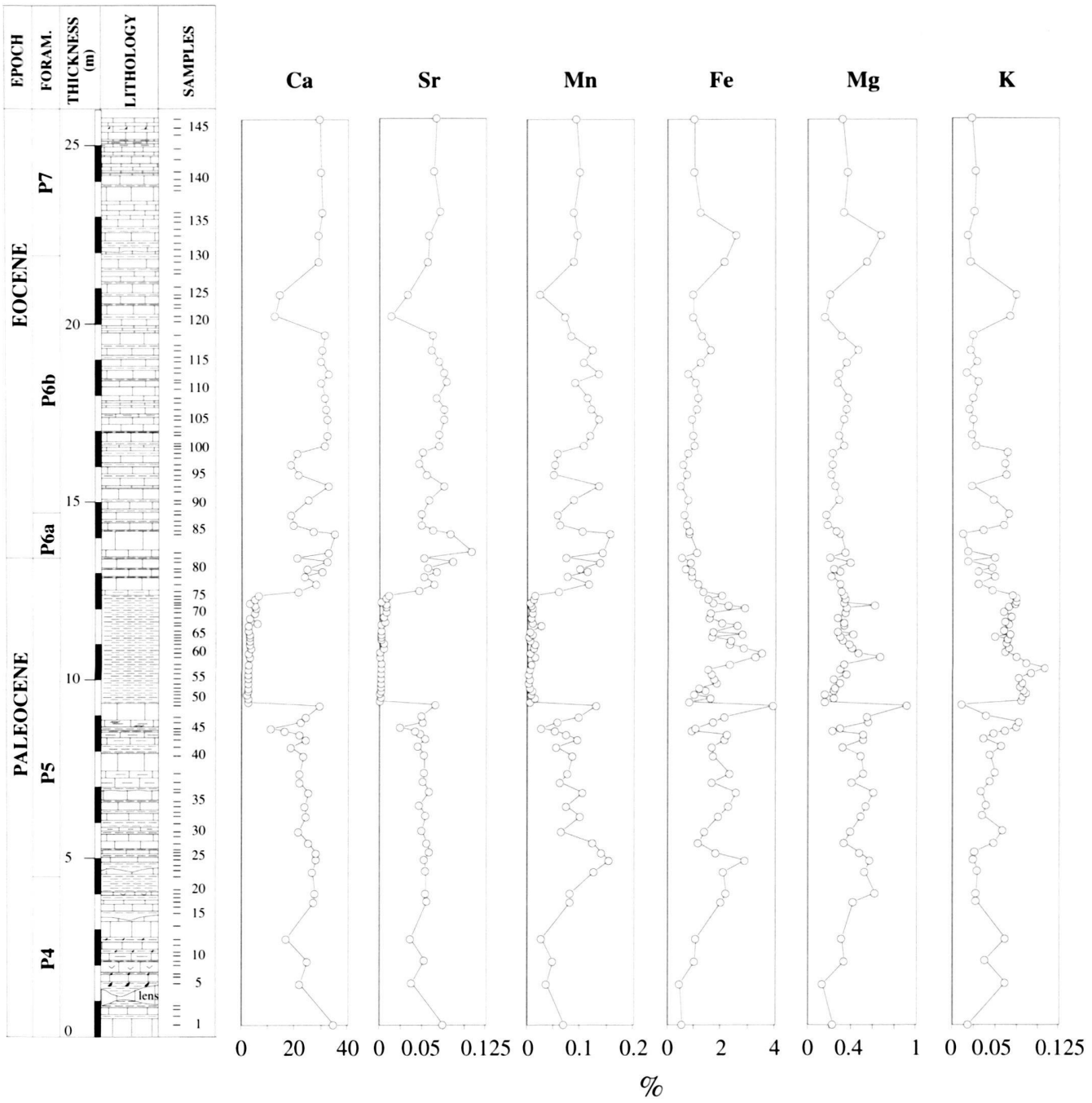

Fig. 9. Chemical elements: variations of Ca, Sr, Mn, Fe, Mg and K across the P/E transition, Trabakua, Spain.

Fig. 8. Grain size changes across the P/E transition, Trabakua, Spain.

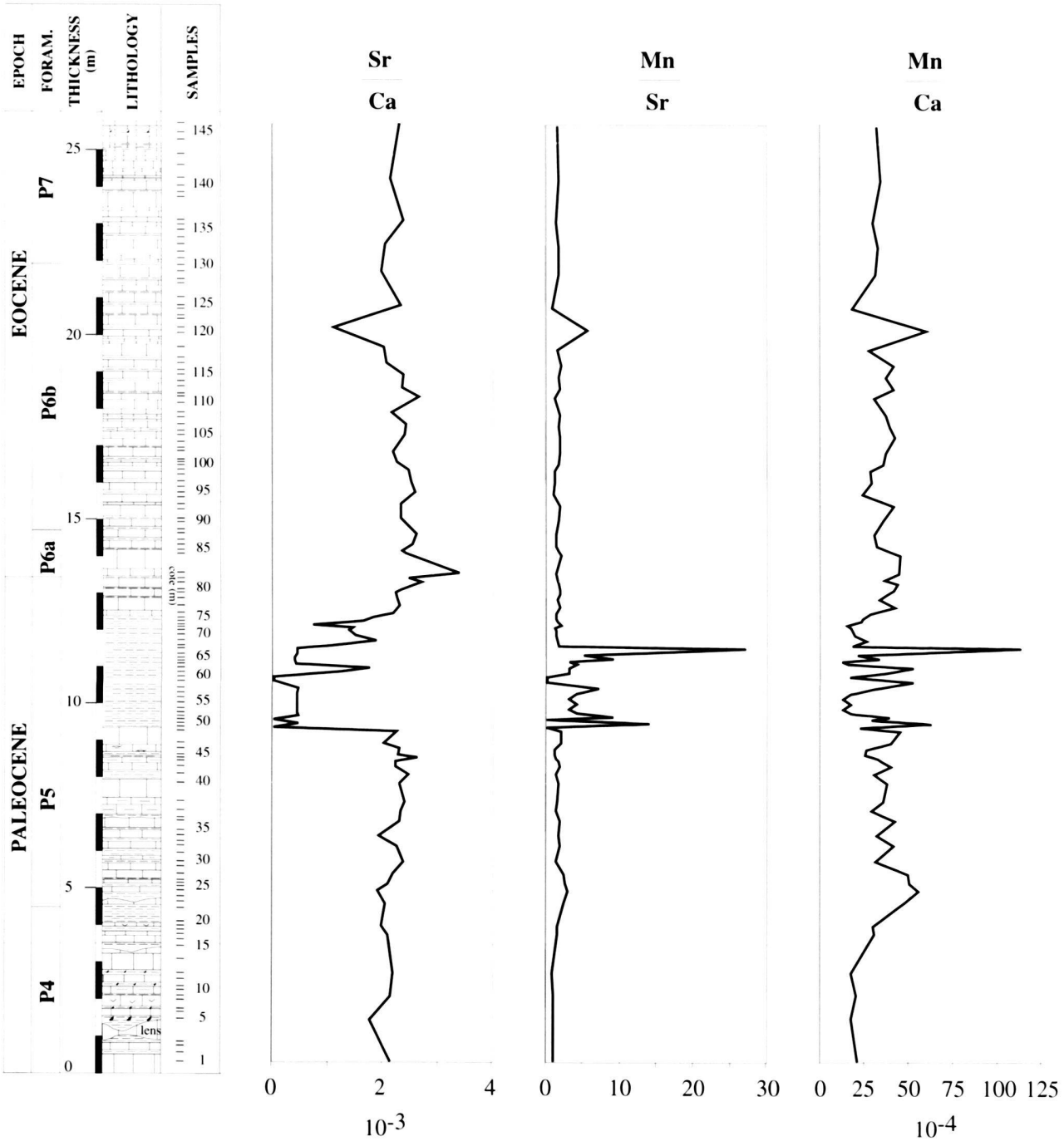

Fig. 10. Sr/Ca, Mn/Sr and Mn/Ca ratios across the P/E transition, Trabakua, Spain.

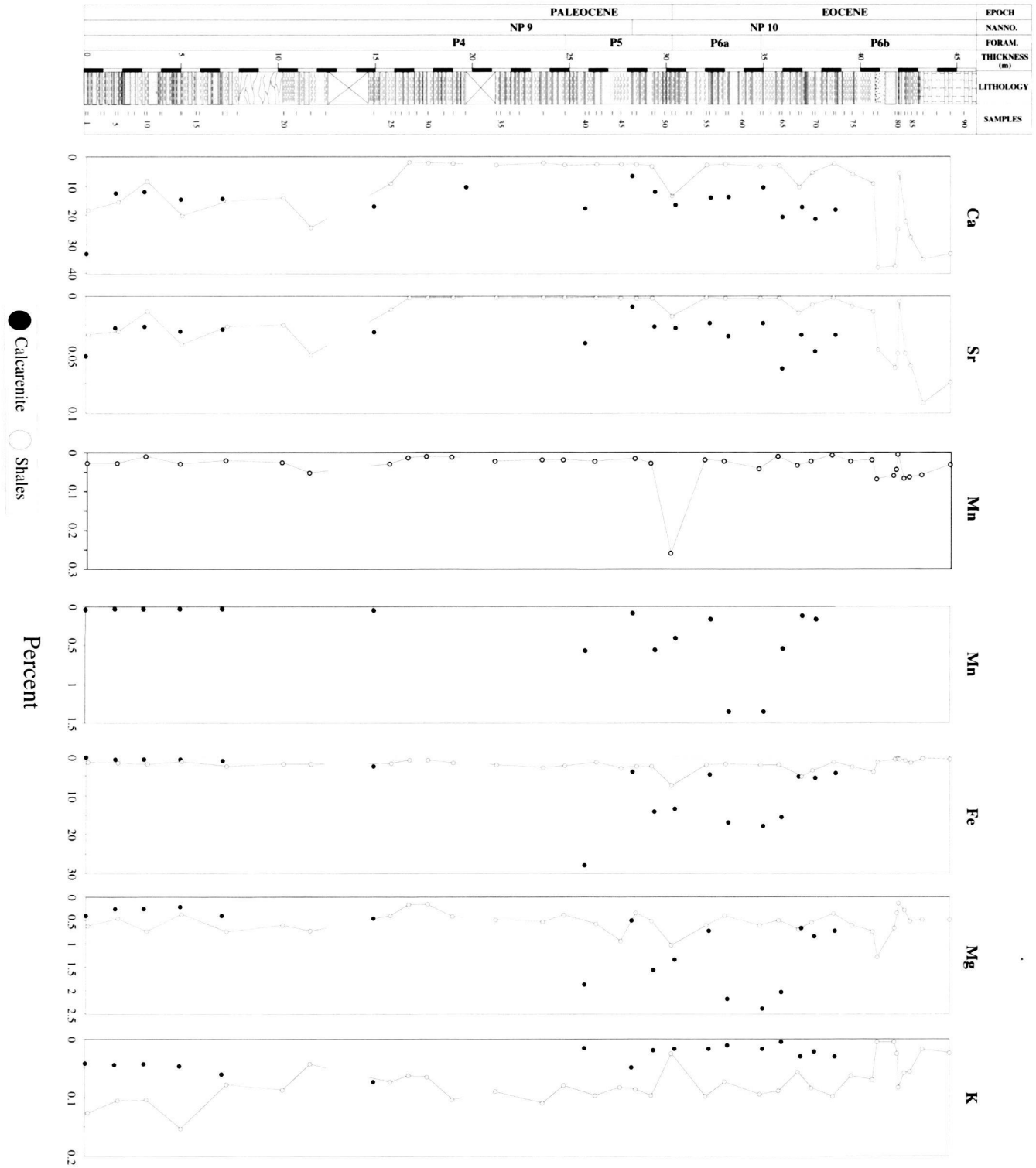

Fig. 11. Chemical elements: variations of Ca, Sr, Mn, Fe, Mg and K across the P/E transition, Ermua, Spain.

decreases to an average of 0.008% within it. Iron increases only slightly (1.8% to 2%) in the clay layer, and decreases to about 1% in the upper marl/limestone interval. Mg averages between 0 and 9.3 m 0.45% and decreases to 0.3% between 9.3 and 26 m. Potassium averages 0.04% except in the clay interval where it reaches 0.07%.

Thus, calcium, strontium and manganese have parallel trends with very low values (near zero) in the clay layer and higher though variable values above and below. Calcium is mainly present in limestone and a decrease to near zero in the clay layer coincides with the decrease in carbonates in this interval (9.3 to 12.3 m). Strontium co-precipitates frequently with aragonite and calcite (Handbook of Geochemistry 1978) and the parallel trend indicates that Sr is associated with calcium in the carbonate fraction. The higher Mn abundance in carbonate rocks is probably derived from diagenetic mobilization of Mn under reducing conditions. The decrease of Mn associated with the decrease of Ca and Sr in the clay interval may indicate significant changes in the reducing conditions during sediment deposition. The ratios of Mn/Sr and Mn/Ca which are very high in the clay interval (Fig. 10) indicate probably an increase of Mn during the Paleocene-Eocene transition. The origin of this manganese could be linked to the increase of the volcanic activity in the North Atlantic during this period (Ritchie & Hitchen 1996).

Magnesium is present in the sediments mainly in phyllosilicates, such as chlorite. The decrease in Mg in the clay layer corresponds to a decrease in chlorite as described in the discussion of the clay minerals (Fig. 3). Potassium in carbonate sediments is almost exclusively contained in the non-carbonate fraction. In the Trabakua Pass section, the K fraction is contained within the siliceous detritus that is present in marls and limestones above and below the clay layer. Within the clay layer, the K fraction is primarily a function of the clay mineral content and secondarily the amount of K-feldspar.

Detrital influx plays an important role in the supply of K, Mg and Fe to the ocean sediments. The increase of these elements across the Paleocene-Eocene transition is due to the increased detrital accumulation in this interval. Major changes in these minerals associated with clay deposition suggest changes in sediments source and/or oceanic circulation.

Ermua

Significant changes occur throughout the Ermua section in all major components (Fig. 11). In the calcarenites calcium and strontium values are very constant with respectively an average of 15% and 0.03% throughout the section. In the hemipelagic marls, calcium and strontium average between 0 m and 16 m respectively 16% and 0.03% and decrease drastically in the middle part (16 m to 41 m) with a mean value of 3% and 0.004% respectively. In the upper more massive limestone (41 to 46 m), calcium averages 25% whereas strontium reaches a mean value of 0.06%. Between 0 and 16 m, manganese averages 0.03% in the two lithologies but increases with a mean value of 0.49% only in the calcarenites between 16 m and 41 m. In the upper calcareous sequence, Mn has a mean value of 0.06%. Potassium decreases from an average of 0.05% below the middle part to an average of 0.02% in it in the calcarenites and from a mean value of 0.1% to 0.08% in the hemipelagic marls. Iron and magnesium average 0.54% and 2.4% respectively in the marls throughout the section. In the calcarenites Mg and Fe increase strongly between 25 m and 39 m from a mean value of 0.33% and 1% to 1.3% and 11% respectively. In the upper massive limestone, K, Mg and Fe reach an average of 0.03%, 0.57% and 0.94% respectively.

Thus, calcium, strontium and manganese have parallel trends in the hemipelagic marls with very low values between 16 m and 41 m and higher though variable values above and below. Calcium decreases to 2% in the middle part coinciding with the decrease in carbonates in this interval (16 m to 41 m). Strontium is associated with calcium in the carbonate fraction and manganese is one of the few minor elements which is more abundant in carbonates than in the detrital fraction.

The calcarenites seem not affected by the decrease of the carbonate sedimentation observed in the marls. Between 25 m and 39 m Fe and Mg increase strongly in the sandstones. The presence of pyrite and goethite described in the bulk rock analyses and the presence of low oxygen tolerant benthic foraminifera indicate low-oxygen environment and explain the very high content of iron. High magnesium content is linked to the increase of chlorite described in clay minerals (Fig. 4) during this interval and its origin is detrital.

Discussion

The P/E transition is globally characterized by a mass extinction in benthic foraminifera, diversification in planktic foraminifera, an abrupt negative $\delta\ ^{13}C$ excursion, a decrease in calcite, an increase in detrital minerals and negative anomalies in Sr and Mn, all of which are present also in the Trabakua section. Moreover, the Trabakua clay layer is more expanded than in deep-sea sections where this interval is concentrated in a few to a few tens of centimeters, However, this interval seems still to be condensed at Trabakua as suggested by the presence of glauconite. Isotopic, geochemical and mineralogical bulk rock analyses of the P-E transition at Trabakua give similar results as those obtained at Caravaca and Alamedilla, located in the Tethyan Realm (Fig. 12). At the coeval Ermua section, these characteristic trends can not be identified (Fig. 12). The turbiditic sedimentation with its low content of carbo-

Fig. 12. Biostratigraphic correlation between Trabakua and Ermua, Atlantic realm and Alamedilla and Caravaca, Tethyan realm. Correlations are based on planktic foraminiferal datum events. The shaded interval corresponds to the carbon-13 isotopic excursion. The Alamedilla data are from Lu et al. (1996). The Caravaca data are from Ortiz (1996).

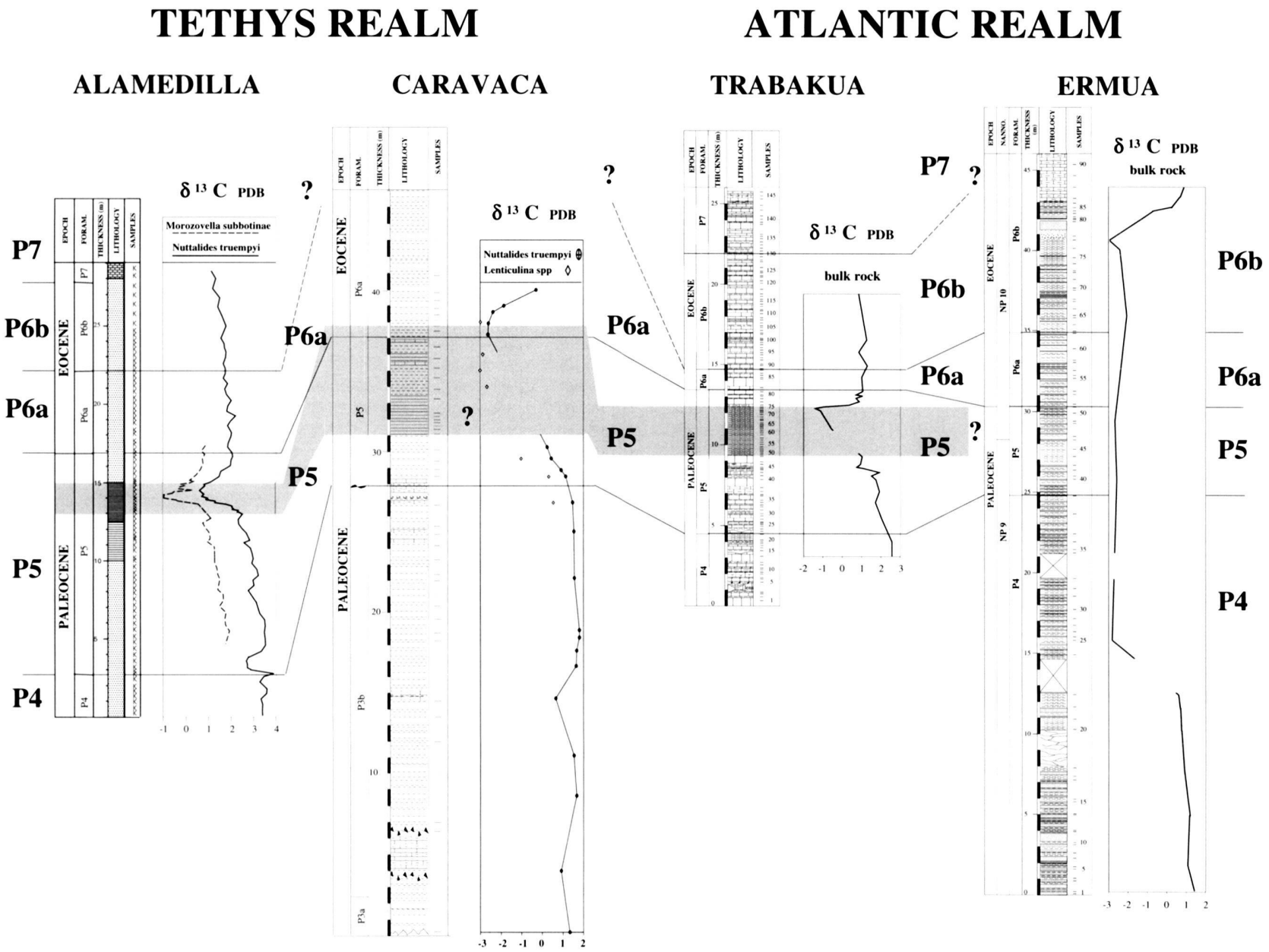
TETHYS REALM
ATLANTIC REALM
ALAMEDILLA
CARAVACA
TRABAKUA
ERMUA
δ 13 C PDB
Morozovella subbotinae
Nuttalides truempyi
Lenticulina spp
bulk rock
EPOCH
FORAM.
NANNO.
THICKNESS (m)
LITHOLOGY
SAMPLES
EOCENE
PALEOCENE
P7
P6b
P6a
P5
P4
P3b
P3a
NP 10
NP 9
?

nates and high content of clays in the hemipelagic marls associated with organic matter seems to obscure or obliterate the isotopic and geochemical signals.

Stable isotope and biostratigraphic data show that the Trabakua section is relatively complete (see also Orue-Etxebarria et al. 1996). During the latest Paleocene (Zone P5), the oceanic carbon reservoir changed dramatically, beginning with a gradual decrease by 1.0‰ of $\delta^{13}C$ values in the lower part of Zone P5, followed by a 3‰ decrease in the clay layer in the upper Zone P5 interval. In the limestone overlying the clay layer, $\delta^{13}C$ values rapidly increase by 2.5‰ and remain steady upsection. The decrease in $\delta^{13}C$ values in the clay layer coincides with a reduction in carbonate to near zero. A similar isotopic profile has been observed in the Alamedilla section of southern Spain (Fig. 12) where Lu et al. (1996), first noted that the rapid excursion in the clay is preceded by a gradual prelude decrease and followed by a gradual recovery. The gradual prelude decrease, rapid excursion and gradual recovery are accompanied by similar trends in calcite concentrations in sediments (Fig. 6). The concomitant decrease in $\delta^{13}C$ and calcite values can be explained by a decrease in primary productivity. Detrital influx, particulary quartz, plagioclase, K-feldspar, phyllosilicates, increased in the clay interval whereas grain size decreased. These changes in detrital influx suggest variations in source rocks and in the intensity of weathering and erosion. This oceanographic event is observed globally and is accompanied by a major mass extinction in benthic foraminifera (~ 50% species extinct) and a major faunal turnover in planktic foraminifera (e.g. Thomas 1990; Lu & Keller 1995a, 1995b; Lu et al. 1996; Ortiz 1996; Thomas & Shackleton 1996).

Clues to environmental conditions in the Pyreneean basin during the P-E transition can be gleaned from clay minerals. Clay mineral assemblages, if not altered by deep burial, reflect continental morphology and tectonic activity linked to the structural evolution of the margins, as well as climatic evolution and associated variations of atmospheric and/or marine circulation (Robert & Chamley 1987). Moreover, detrital clay mineral compositions in marine sediments record qualitative signals of regional climatic changes (Millot 1970; Chamley 1989). For instance, kaolinite forms abundantly in soils of intertropical land masses characterized by warm, humid climates. Kaolinite abundance increases toward the Equator in all oceanic basins (Chamley 1989). In contrast, detrital chlorite increases toward cold latitudinal zones parallel to the decrease of continental hydrolysis. Chlorite forms also in cold and dry or frozen regions. Mica tends to increase toward high latitudes, similar to chlorite, which reflects decreased chemical weathering and increased mechanical erosion under cold climatic conditions (Chamley 1989).

Although clays in the Trabakua and Ermua sections have undergone significant burial diagenesis, mica and chlorite are partly detrital, indicating that the adjacent areas were characterized by a dry climate. Sediments at Ermua contain higher kaolinite percentages in marls (15–23%) than at Trabakua where kaolinite does not exceed 8%. At Ermua, in calcarenites which contain reworked shallow-water carbonate platform sediments, kaolinite reaches a maximum of 10% and averages 7%. These data suggest that the kaolinite is transported by oceanic currents and does not come from adjacent land areas. In the Zumaya section, kaolinite first appears 6 m below the Paleocene/Eocene transition and rapidly disappears upward. The presence of kaolinite close to coastal areas and the extinction of benthic foraminifera are likely to be the result of a global turnover in oceanic circulation (Adatte et al. 1995).

Trabakua Pass section: a potential Paleocene/Eocene GSSP?

The Paleocene/Eocene boundary is usually placed at the P5/P6 (Berggren et al. 1995) zonal boundary by planktic foraminiferal specialists. Calcareous nannoplankton specialists generally use the NP9/NP10 zonal boundary. Designation of suitable markers for this boundary and the problems associated with chosing an oceanographic event as marker, are currently investigated and examined by workers of the IGCP Project 308 (Paleocene/Eocene Boundary Events in Time and Space) (see Berggren & Aubry 1995; Aubry et al. 1995; Berggren et al. 1995).

A potential GSSP candidate section for the P/E boundary has to fulfil certain conditions suggested by the International Commission on Stratigraphy. These conditions include: a) easy access, b) open marine sedimentation, c) continuous sedimentation across the boundary, d) absence of synsedimentary and tectonic disturbances, e) absence of redeposition or diagenetic alteration, f) abundance and diversity of well preserved fossils, and g) good magnetostratigraphic and isotopic records (Remane et al. 1997).

Previous reports on the Trabakua section concluded that most of these conditions were satisfied and that Trabakua could be considered as suitable global stratotype section and point (Coccioni et al. 1994; Orue-Etxebarria et al. 1996). Our study partly concurs with this assessment insofar as the global biostratigraphic, geochemical and isotopic markers are present. However, the section is not ideal for several reasons. 1) Microfossils are very poorly preserved, phosphatized, recrystallized or completely replaced by diagenetic calcite. The poor preservation and often sporadic occurrence makes it difficult to positively identify species. This is a serious problem which we observed in trying to reproduce the biostratigraphies of Coccioni et al. (1994) and Orue-Etxebarria et al. (1996) in the same section. As stratotype, Trabakua would necessarily cause problems when correlating this section with well-preserved faunas and floras of other sections. Moreover, no paleotemperature signals can be obtained from the recrystallized calcite of the Trabakua section. 2) Sedimentation across the clay layer may be discontinuous, as suggested by the presence of glauconite. 3) The clays are affected by deep burial diagenesis corresponding approximately to the upper part of Zone 3 (> 100 °C) of Kübler et al. (1979). We conclude therefore that the Trabakua Pass section is not an optimal stratotype for the Paleocene-Eocene transition.

Conclusions

Expanded sedimentary records from Trabakua, Spain, reveal unique faunal, isotopic, geochemical, mineralogical and sedimentary compositional changes across the Paleocene-Eocene (P-E) transition. Unlike in the open oceans, the Trabakua section exhibits a gradual decrease of 1.3‰ in $\delta^{13}C$ values prior to the rapid $\delta^{13}C$ excursion. Associated with the $\delta^{13}C$ excursion is a decrease in calcite preservation, increase in detrital content and reduction in the grain size.

These major changes across the P/E transition are explained by a reduced intensity of sea-surface circulation with a concomitant decrease in the primary biological productivity. The decline in carbonate productivity is partially reflected in the negative shift of $\delta^{13}C$ values which occurred exactly at the same time.

The increase in detrital minerals together with a decrease of grain sizes across the P/E transition indicate changes of global oceanic currents and/or reduction of the intensity of atmospheric circulation probably associated with changes in sediments sources.

Acknowledgements

We thank X. Arostegui, X. Orue-Etxebarria and V. Pujalte from the University of Bilbao, Spain, for guiding us in the field. Thanks to C. Beck for conducting geochemical analyses and J. Richard for conducting X-ray preparations at the laboratory of mineralogy and petrology, University of Neuchâtel, Switzerland. We thank also J. Remane, Institute of Geology, Neuchâtel, A–C. Bartolini from the stable isotope laboratory at the University of Lausanne, Switzerland for providing important comments and suggestions on an early draft. We sincerely thank H.P Luterbacher (Tübingen) and X. Orue-Etxebarria (Bilbao) for a stimulating review of the manuscript.

This study was supported by Swiss National Foundation, N° 2100–043450.95/1

REFERENCES

ADATTE, T., LU, G. & KELLER, G. 1995: Clay mineral correlation across the Paleocene-Eocene boundary: evidence for global paleo-oceanographic turnover. GSA 1995, annual meeting, New Orleans, USA, abstract p. 405.

ANGORI, E. & MONECHI, S. 1996: High resolution calcareous nannofossil biostratigraphy across the Paleocene/Eocene boundary at Caravaca (southern Spain). Israel. J. of Earth Sc. 44, 197–206.

AUBRY, M.P., BERGGREN, W.A., STOTT, L.D. & SINHA, A. 1995: The upper Paleocene-lower Eocene stratigraphic record and the Paleocene-Eocene boundary isotope excursion: implications for geochronology. In Correlation of the Early Paleogene in Northwestern Europe. (Ed. by KNOX, R.O.B., CORFIELD, R.M. & DUNNAY, R.E.) London: Special Publication of the Geological Society, 1996, 353–380.

AUBRY, M.P. 1996: Towards an Upper Paleocene-Lower Eocene High Resolution Stratigraphy Based on Calcareous Nannofossil Stratigraphy. Israel. J. of Earth Sc. 44, 239–253.

AXELROD, D.I. 1992: What is an equable climate? Palaeogeogr., Palaeoclimatol., Palaeoecol. 91, 1–12.

BARTOLINI, A.C, BAUMGARTNER, P.O. & HUNZIKER, J. 1996: Middle and Late Jurassic carbon stable-isotope stratigraphy and radiolarite sedimentation of the Umbria-March Basin (Central Italy). Eclogae geol. Helv. 89/2, 811–844.

BERGGREN, W.A. & AUBRY, M.P. 1995: A Late Paleocene-early Eocene NW European and North Sea magnetobiochronology correlation network: A sequence stratigraphic network. In Correlation of the Early Paleogene in Northwestern Europe. (Ed by KNOX, R.O.B., CORFIELD, R.M. & DUNNAY, R.E.) London: Special Publication of the Geological Society, 1996, 309–352.

BERGGREN, W.A, KENT, D.V., SWISHER, C.C. & AUBRY, M.P. 1995: A revised Cenozoic geochronology and chronostratigraphy. In Geochronology, time scale and global stratigraphy correlation. (Ed. by BERGGREN, W.A., KENT, D.V., AUBRY, M.P. & J. HARDENBOL) Tulsa, Oklahoma, USA: SEPM Special Publication N°54, 129–212.

BERGGREN, W.A & MILLER, K.G. 1988: Paleogene planktonic foraminiferal biostratigraphy and magnetobiostratigraphy. Micropaleontology 34, 362–380.

BOLES, J.R. & FRANCKS, S.G. 1979: Clay diagenesis in Wilcox sandstones of Southwest Texas: implications of smectite diagenesis on sandstone cementation. J. Sed. Petr. 49, 55–70.

BRALOWER, T.J., ZACHOS, J.C., THOMAS, E., PARROW, M., PAUL, C.K., KELLY, D.C., PREMOLI SILVA, I., SLITER, W.V. & LOHMANN, K.C. 1995: Late Paleocene to Eocene paleoceanography of the equatorial Pacific Ocean: Stable isotopes recorded at Ocean Drilling Program Site 865, Allison Guyot. Paleoc. 10, 841–865.

BYBELL, L.M. & SELF-TRAIL, J.M. 1995: Evolutionary, Biostratigraphic, and Taxonomic Study of Calcareous Nannofossils from a Continous Paleocene-Eocene Boundary Section in New-Jersey. U.S. Geol. Survey Prof. Paper. 1554, 1–36.

CALVERT, S.E. 1987. Oceanographic controls on the accumulation of organic matter in marine sediments. In Marine petroleum source rocks. (Ed. by BROOKS, J. & FLEETS, A.J.). Geol. Soc. London Spec. Publ.

CANUDO, J.I., KELLER, G., MOLINA, E. & ORTIZ, N. 1995: Planktic foraminiferal turnover and $\delta^{13}C$ isotopes across the Paleocene-Eocene transition at Caravaca and Zumaya, Spain. Palaeogeogr., Palaeoclimatol., Palaeoecol. 114, 75–100.

CHAMLEY, H. 1989: Clay Sedimentology. Springer-Verlag. Berlin–Heidelberg, 623.

COCCIONI, R., DI LEO, R., GALEOTTI, S. & MONECHI, S. 1994: Integrated biostratigraphy and benthic foraminiferal faunal turnover across the Paleocene-Eocene boundary at Trabakua Pass section, Northern Spain. Palaeopelagos 4, 87–100.

ERBA, INSTRUMENTS CARLO. 1990: Instruction manual, eager 2000. (Ed. by FISONS).

FERRERO, J. 1965: Dosage des principaux minéraux des roches par diffraction de Rayon X. Rapport C.F.P (Bordeaux), inédit.

– 1966: Nouvelle méthode empirique pour le dosage des minéraux par diffraction R.X. Rapport C.F.P (Bordeaux), inédit, 26.

GINGERICH, P.D. 1980: Evolutionary patterns in early Cenozoic mammals. Ann. Rev. Earth Planet. Sci. 8, 407–424.

– 1986: Evolution and fossil record: patterns, rates and processes. Canadian Journal of Zoology 65, 1053–1060.

HANDBOOK OF GEOCHEMISTRY 1978: Springer-Verlag. Berlin–Heidelberg–New York, 1200.

HOWER, J., ESLINGER, E.V., HOWER, M.E. & PERRY, E.A. 1976: Mechanisms of burial metamorphism of argillaceous sediment: 1. Mineralogical and chemical evidence. Geol. Soc. Amer., Bull. 87, 725–737.

JANTSCHIK, R., NYFFELER, F. & DONARD, O.F.X. 1992: Marine particle size measurement with a stream-scanning laser system. Marine Geology 106, 239–250.

KATZ, M.E. & MILLER, K.G. 1991: Early Paleogene benthic foraminiferal assemblages and stable isotopes in the Southern Ocean. Proc. ODP, Sci. Res. 114, 481–512.

KENNETT, J.P. & STOTT, L.D. 1990: Proteus and Proto-Oceanus: Paleogene oceans as revealed from Antarctica stable isotopic results. In Proc. ODP, Sci. Res. 113, 865–879.

– 1991: Abrupt deep-sea warming, palaeoceanographic changes and benthic extinctions at the end of the Paleocene. Nature 353, 225–229.

KLOOTWIJK, C.T., GEE, J.S., PEIRCE, J.W., SMITH, G.M. & MCFADDEN, P.L. 1992: An early India-Asia contact: Paleomagnetic constraints from Ninetyeast Ridge, ODP Leg 121. Geology 20, 395–398.

KLUG, H.P. & ALEXANDER, L. 1974: X-ray Diffraction Procedures for Polycrystalline and Amorphous Materials. (Ed. by JOHN WILEY and SONS, INC.). New York.

KOCH, P.L., ZACHOS, J.C. & GINGERICH, P.D. 1992: Correlation between isotope records in marine and continental carbon reservoir near the Paleocene/Eocene boundary. Nature 358, 319–322.

KÜBLER, B. 1983: Dosage quantitatif des minéraux majeurs des roches sédimentaires par diffraction X. Cahier de l'institut de Géologie de Neuchâtel Série AX N°1.1 & 1.2.

– 1987: Cristallinité de l'illite, méthodes normalisées de préparations, méthodes normalisées de mesures. Cahiers de l'Institut de Géologie de Neuchâtel Série ADX, 1–8.

KÜBLER, B., PITTION, J.C., HERIOUX, Y., CHAROLLAIS, J. & WEIDMANN, M. 1979: Sur le pouvoir réflecteur de la vitrinite dans quelques roches du Jura, de la Molasse et des Nappes préalpines, helvétiques et penniques (Suisse occidentale et Haute-Savoie). Eclogae geol. Helv. 72, 347–373.

LU, G. & KELLER, G. 1993: The Paleocene-Eocene transition in the Antarctic Indian Ocean: inference from planktic foraminifera. Mar. Micropaleontol. 21, 101–142.

– 1995a: Planktic foraminiferal faunal turnovers in the subtropical Pacific during the late Paleocene to early Eocene. J. Foram. Res. 26, 97–116.

– 1995b: Ecological stasis and saltation: species richness change in planktic foraminifera during the late Paleocene to early Eocene, DSDP Site 577. Palaeogeogr., Palaeoclimatol., Palaeoecol. 117, 211–227.

LU, G., KELLER, G., ADATTE, T. & BENJAMINI, C. 1995: Abrupt change in the upwelling system along the southern margin of the Tethys during the Paleocene-Eocene transition event, Israel. J. Earth Sci. 44, 185–195.

LU, G., KELLER, G., ADATTE, T., ORTIZ, N. & MOLINA, E. 1996: Long-term (10^5) or short-term (10^3) $\delta\ ^{13}C$ excursion near the Palaeocene-Eocene transition: evidence from the Tethys. Terra Nova 8, 347–355.

MAGARITZ, M., BENJAMINI, C., KELLER, G. & MOSHKOVITZ, S. 1992: Early diagenetic isotopic signal at the Cretaceous/Tertiary boundary, Israel. Palaeogeogr., Palaeoclimato., Palaeoecol. 91, 291–304.

MARTINI, E. 1971: Standard Tertiary and Quaternary calcareous nannoplankton zonation. In Proc. 2nd Planktonic Conference. (Ed by FARINACCI, A.). Roma: Tecnoscienza, 739–785.

MCCREA, J.M. 1950: On the Isotopic Chemistry of the Carbonates and a Paleotemperatures Scale. Jour. Chem. Phys. 18, 849–857.

MILLER, K.G., JANECEK, T.R., KATZ, M.E. & KEIL, D.J. 1987: Abyssal circulation and benthic foraminiferal changes near the Paleocen-Eocene boundary. Paleoceanography. 2, 741–761.

MILLOT, G. 1970: Geology of Clays. Springer Verlag. Berlin, Heidelberg, New York, 499.

MOORE, D. & REYNOLDS, R. 1989: X-Ray-diffraction and the identification and analysis of clay-minerals. Oxford University Press, 332.

MUFFLER, L.P.J. & WHITE, D.E. 1969: Active metamorphism of Upper Cenozoic sediments in the Salton Sea geothermal fild and the Salton Trough, southeastern California. Geol. Soc. Amer., Bull. 80, 157–182.

O'CONNELL, S.B.O. 1990: Variations in upper Cretaceous and Cenozoic calcium carbonate percentages, Maud Rise Weddell Sea. In: Proc. ODP, Sci. Res. 113, 971–984.

OBERHÄNSLI, H. 1992: The Influence of the Tethys on the bottom waters of the early Tertiary ocean. In The Antarctic Paleoenvironment: A Perspective on Global Change. (Ed. by KENNETT, J.P.), 167–184.

OBERHÄNSLI, H. & HSÜ, K.J. 1986: Paleocene-Eocene paleoceanography. In Mesozoic and Cenozoic Oceans. Geodynamic Series. 15, 85–100.

OINUMA, K., SHIMODA, S. & SUDO, T. 1972: Triangular diagrams of surveying chemical compositions of chlorites. J. Tokyo Univ. 15, 1–13.

ORTIZ, N. 1996: Differential patterns of benthic foraminiferal extinctions near the Paleocene/Eocene boundary in the North Atlantic and the western Tethys. Mar. Micropaleontol. 26, 341–359.

ORUE-ETXEBARRIA, X., APELLANIZ, E., BACETA, J.I., COCCIONI, R., DI LEO, R., DINARES-TURELL, S., GALEOTTI, S., MONECHI, S., NUNEZ-BETELU, K., PARES, J.M., PAYROS, A., PUJALTE, V., SAMSO, J.M., SERRA-KIEL, J., SCHMITZ, B. & TOSQUELLA, J. 1996: Physical and biostratigraphic analysis of two prospective Paleocene-Eocene Boundary Stratotypes in the intermediate-deep water Basque Basin, western Pyrenees: The Trabakua Pass and Ermua sections. N. Jb. Geol. Paläont., Abh. 200, 1–64.

PAK, D.K. & MILLER, K.G. 1992: Paleocene to Eocene benthic foraminiferal isotopes and assemblages:implications for deepwater circulation. Paleoceanography. 7, 741–761.

PERRY, E. & HOWER, J. 1970: Burial diagenesis in Gulf Coast pelitic sediments. Clays and clay minerals 18, 165–177.

PLAZIAT, J.C. 1981: Late Cretaceous to late Eocene Paleogeographic evolution of southwest Europe. Palaeogeogr., Palaeoclimatol., Palaeoecol. 36, 263–320.

PUJALTE, V., BACETA, J.I., DINARÈS-TURELL, J., ORUE-ETXEBARRIA, X. PARES, J.M. & PAYROS, A. 1995: Biostratigraphic and magnetostratigraphic intercalibration of latest Cretaceous and Paleocene depositional sequences from the deep-water Basque Basin, Western Pyrenees, Spain. Earth and Planetary Sci. Lett. 136, 17–30.

PUJALTE, V., BACETA, J.I., PAYROS, A., ORUE-ETXEBARRIA, X. & SERRA-KIEL, J. 1994: Late Cretaceous-middle Eocene sequence stratigraphy and biostratigraphy of SW and W Pyrenees (Pamplona and Basque Basin, Spain. Guide-book of a field seminar of the Groupe d'étude du Paléocène and IGCP 286, 118.

PUJALTE, V., ROBLES, S., BACETA, J. & ORUE-ETXEBARRIA, X. 1992: Latest Cretaceous-early Eocene sedimentation in the deep-water Basque Basin (northern Spain): Eustatic and Tectonic influences. Field Trip guide book of the International Symposium on "Mesozoic and Cenozoic Sequence Stratigraphy of European Basins". Dijon, France.

PUJALTE, V., ROBLES, S., ROBADOR, A., BACETA, J. & ORUE-ETXEBARRIA, X. 1993: Shelf-to-Basin Paleocene Palaeogeography and depositional sequences, Western Pyrenees, North Spain. In Sequence Stratigraphy and Facies Association. (Ed. by POSAMENTIER, H.W., SUMMERHAYES, C.P., HAQ, B.U. & ALLEN, G.P). Special Publication Int. Assoc. Sedimentologists. 18, 369–395.

RAYMO, M.E., RUDDIMAN, W.F. 1992: Tectonic forcing of Late Cenozoic climate. Nature 359, 117–122.

REA, D.K., ZACHOS, J.C., OWEN, R.M. & GINGERICH, P.D. 1990: Global changes at the Paleocene-Eocene boundary: climate and evolutionary consequences of tectonic events. Palaeogeogr., Palaeoclimatol., Palaeoecol. 79, 117–128.

REMANE, J., BASSETT, M.G., COWIE, J.W., GOHRBANDT, H.K., LANE, H.R., MICHELSEN, O. & WANG, N. 1996: Revised guidelines for the establishment of global chronostratigraphic standards by the international commission on stratigraphy (ICS). Episodes 19/3, 77–81.

RITCHIE, J.D.& HITCHEN, K. 1996: Early Paleogene offshore igneous activity to the northwest of the UK margin and its relationship to the North Atlantic Igneous Province. In Correlation of the Early Paleogene in Northwest Europe. (Ed. by KNOX, R.W., CORFIELD, R.M. & DUNAY, R.E.) London. The Geological Society, 1996, 63–78.

ROBERT, C. & CHAMLEY, H. 1987: Cenozoic evolution of continental humidity and paleoenvironment, deduced from the kaolinite content of oceanic sediments. Paleogeogr., Paleoclimatol., Paleoecol. 60, 171–187.

ROBERT, C. & KENNETT, J.P. 1994: Antarctic subtropical humid episode at the Paleocene-Eocene boundary; Clay-mineral evidence. Geology 22, 211–214.

SCHMITZ, B., SPEIJER, R.P. & AUBRY, M.P. 1995: Latest Paleocene benthic extinction event on the southern Tethyan shelf (Egypt): Foraminiferal stable isotopic $\delta\ ^{13}C$ and $\delta\ ^{18}O$ records. Geology 24, 347–350.

SELVERSTONE, J. & GUTZLER, D.S. 1993: Post-125 Ma carbon storage associated with continent-continent collision. Geology 21, 885–888.

SPEIJER, R.P. 1994a: Extinction and recovery patterns in benthic foraminiferal paleocommunities across the Cretaceous/Paleogene and Paleocene/Eocene boundaries. Geologica Ultraiectina, University of Utrecht.

– 1994b: The late Paleocene benthic foraminiferal extinction as observed in the Middle East. Bull. Soc. belge Géol. 103, 267–280.

STOTT, L.D. 1992: Higher temperatures and lower oceanic pCO2: a climate enigma at the end of the Paleocene Epoch. Paleoceanography. 7, 395–404.

STOTT L.D., SINHA, A. TIRY, M. AUBRY, M.P. & BERGGREN, W.A. in press: The transfer of $\delta\ ^{12}C$ changes from the ocean to the terrestrial biosphere across the Paleocene-Eocene boundary: criteria for terrestrial-marine correlations. Geol. Soc. Spec. Publ.

THOMAS, E. 1990: Late Cretaceous through Neogene deep-sea benthic foraminifers (Maud Rise, Weddell Sea, Antarctica). In: Proc. ODP. Sci. Results 113, 571–594.

THOMAS, E. & SHACKLETON, N.J. 1996: The latest Palaeocene benthic foraminiferal extinction and stable isotope anomalies. J. Geol. Soc. London 101, 421–441.

VEIZER, J. 1983: Trace elements and isotopes in sedimentary carbonates. In Carbonates: mineralogy and chemistry (Ed. by REEDER, R.J). Min. Soc. Am. Rev. Min. 11, 265–299.

VERARDO, D.J., FROELICH, P.N. & MCINTYRE, A. 1990: Determination of organic carbon and nitrogen in marine sediments using the Carlo Erba NA-1500 Analyzer. Deep Sea Research 57, 157–165.

WEAVER, C.E. 1989: Clays, Muds, and Shales. Elsevier Science Publishers B.V. Amsterdam, 819.

WEI, W. & ZHONG, S. 1996: Taxonomy and magnetobiochronology of Tribrachiatus and Rhomboaster, two genera of calcareous nannofossils. J. Paleont. 70, 7–22.

WING, S.L., BOWN, T.M. & OBRADOVICH, J.D. 1991: Early Eocene biotic and climatic change in interior western America. Geology 19, 1189–1192.

WING, S.L. & GREENWOOD, D.L. 1993: Fossils and fossil climate: The case for equable continental interiors in the Eocene. Royal Soc. London Philo. Trans. ser. 341, 243–252.

Manuscript received February 22, 1997
Revision accepted June 8, 1997